厚生労働科学研究費補助金（第３次対がん総合戦略研究事業）

分担研究報告書

ユーイング肉腫における新規膜抗原・分泌蛋白の探索

分担研究者　野阪 哲哉　三重大学大学院 医学系研究科
病態解明医学講座 感染症制御医学分野　教授

研究要旨

ユーイング肉腫（Ewing sarcoma）は若年者に好発する骨腫瘍である。化学療法の発達により予後は改善されつつあるが、依然不良であり、早期診断が望まれる。当研究ではシグナルシークエンストラップ法を用いて、ユーイング肉腫に特異的な新規膜抗原や分泌蛋白のスクリーニングを行った。

A. 研究目的

ユーイング肉腫は 1921 年、ユーイングによって報告された高悪性度小円形細胞肉腫で、5-15 歳で発症し、骨肉腫よりも若年者に好発する傾向がある。大腿骨、骨盤、肋骨に好発し、画像的には玉ねぎの皮様と表現される骨膜反応を伴った骨吸収破壊像が特徴的である。ユーイング肉腫の細胞起源は不明であり、骨の腫瘍であるにもかかわらず軟部への進展が速い。放射線や化学療法に対する反応はよいが、再発しやすく、骨や肺への転移のため、5 年生存率は 50%程度と悪性度の高い腫瘍である。ユーイング肉腫は、骨を覆っている軟部組織が厚いために早期発見が困難な場合も多く、また、ユーイング肉腫に比較的特異的とされる膜蛋白 MIC2（CD99）は診断の補助にはなるが、完全に特異的というわけではなく、ある種のリンパ腫や横紋筋肉腫、肺小細胞癌の一部でも発現が見られる。したがって、早期診断と鑑別診断の目的で、ユーイング肉腫特異的な分泌蛋白、膜蛋白を同定することが望まれている。

本研究はそのような腫瘍マーカーとなる分子の探索を目的としており、将来的には分子標的療法への応用も視野に入れている。

B. 研究方法

(レトロウイルスを用いたシグナルシークエンストラップ法によるユーイング肉腫特異的分泌蛋白、膜蛋白遺伝子の同定)

当研究代表者らが開発したシグナルシークエンストラップ法 (Kojima T and Kitamura T, Nat Biotechnol 1999) は、IL-3 依存性のマウス血液細胞株 Ba/F3 が活性型 c-mpl によってトランスフォームし、IL-3 非依存性に増殖するようになる性質を応用したものである。即ち、細胞膜に局在できないように細工した活性型 c-mpl 遺伝子との融合遺伝子ライブラリーを作成し、融合遺伝子がシグナルシークエンスを有する場合にのみ、活性型 c-mpl 遺伝子が細胞膜に移行し、Ba/F3 細胞をトランスフォームすることを利用して、シグナルシークエンスをもつ遺伝子を単離するという原理である。ライブラリーの作成に用いる mRNA が由来する細胞を選択することにより、組織特異的な分泌蛋白、膜蛋白遺伝子を単離することが可能となる。研究分担者らはユーイング肉腫由来のヒト細胞株 (SJES-2, SJES-3, SJES-5, SJES-6, SJES-7, SJES-8) を用いて、各々から mRNA を抽出し、それらを等量ずつ混合し、そこからシグナルシークエンストラップ用のライブラリーを作成し、Ba/F3 細胞でスクリーニングを行った。得られたクローンからゲノム DNA を抽出し、ライブラリーの作成に用いたベクター特異的配列を primer にした PCR を行い、増幅された DNA の塩基配列を決定した。ユーイング肉腫の細胞起源に関する定説はないが、間葉系幹細胞由来説や末梢原始神経外胚葉性腫瘍説などが提唱されており、まず、ヒト間葉系幹細胞株から mRNA を抽出し、下記で絞られた遺伝子の発現を RT-PCR で調べる計画である。並行して、候補遺伝子の正常組織での発現パターンも解析する。

(倫理面への配慮)

ここまでの研究ではすでに他所で樹立されたヒトの細胞株を使用しているが、直接の患者検体は使用していない。ヒトの直接の検体を利用する場合は、三重大学の倫理審査委員会の指針に従って該当者に説明を行い、同意書に署名をいただく。

C. 研究結果

レトロウイルス発現系を用いたシグナルシークエンストラップ法にて 81 種類 257 クローンが単離された (別表参照、各遺伝子の左に書かれた数字は単離された頻度を示す)。これら遺伝子の中から、目的の遺伝子を探索する。明らかに組織特異性のない遺伝子や

他の組織の癌細胞で強く発現されているものは、除外し、候補を絞っていく。

D. 考察

これから目的遺伝子を絞り込み、詳細に解析していく予定であるが、疾患特異性のある分子を探索していきたい。現在までのところ、CD99 に似た分子 CD99L2 などの興味深い遺伝子が単離されている。

E. 結論

レトロウイルス発現クローニング法を用いたシグナルシークエンストラップ法にて 6 種のユーイング肉腫細胞株mRNA の混合物から、81 種、257 クローンの遺伝子を単離し、現在解析中である。

F. 健康危険情報

特になし

G. 研究発表

1. 論文発表

1) Ozaki K, Hishiya A, Hatanaka K, Nakajima H, Wang G, Hwu P, Kitamura T, Ozawa K, Leonard WJ, and Nosaka T. (2006) Overexpression of Interleukin 21 induces expansion of hematopoietic progenitor cells. Int J Hematol 84:224-230.

2) Kawashima T, Bao YC, Moon Y, Tonozuka Y, Minoshima Y, Hatori T, Kiyono M, Nosaka T, Nakajima H, Williams DA, and Kitamura T. (2006) Rac 1 and a GTPase-activating protein, MgcRacGAP, are required for nuclear translocation of STAT transcription factors. J Cell Biol 175:937-946.

3)小埜良一、野阪哲哉. MLL 関連白血病の分子病態. 血液・腫瘍科 52(6):615-624,
2006.

2. 学会発表

1)Watanabe-Okochi N, Kitaura J, Harada H, Ono R, Inaba T, Nakajima H, Nosaka T, and Kitamura T. (2006 年 9 月) A BMT model mouse for myelodysplastic syndromes (MDS) and MDS/overt leukemia. 35th Annual Meeting of the International Society of Experimental Hematology.

2)Ono R, Kumagai H, Nakajima H, Tonozuka Y, Hishiya A, Taki T, Hayashi Y, Kiatamura T, and Nosaka T. (2006 年 12 月) MAP kinase activation is essential for the development of acute leukemia by

MLL fusion protein and FLT3 tyrosine kinase mutation. 48th Annual Meeting of the American Society of Hematology.

3)Matsushita H, Nakajima H, Nakamura Y, Tsukamoto H, Tanaka Y, Asai S, Nosaka T, Ando K, and Miyachi H. (2006年12月) C/EBPa and C/EBPe induce manocytic differentiation of myelomonocytic cells with MLL chimeric fusion gene. 48th Annual Meeting of the American Society of Hematology.

4)Watanabe-Okochi N, Kitaura J, Harada H, Ono R, Nakajima H, Nosaka T, Inaba T, and Kitamura T. (2006年12月) A BMT model mice for myelodysplastic syndromes (MDS) and transformation to AML. 48th Annual Meeting of the American Society of Hematology.

5)小埜良一、熊谷英敏、中島秀明、殿塚行雄、菱谷愛、滝智彦、林泰秀、北村俊雄、野阪哲哉. (2006年9月) MLL融合蛋白による多段階発癌モデルマウス：MAP キナーゼの重要性. 第65回日本癌学会学術総会.

6)渡辺直子、北浦次郎、原田浩徳、小埜良一、米野由希子、佐藤均、稲葉俊哉、中島秀明、野阪哲哉、北村俊雄. (2006年10月) AML1点変異はマウスBMTモデルにおいてMDS/AMLを発症させる. 第68回日本血液学会総会.

7)小埜良一、熊谷英敏、中島秀明、殿塚行雄、菱谷愛、滝智彦、林泰秀、北村俊雄、野阪哲哉. (2006年10月) MLL融合蛋白による多段階発癌にはMAPキナーゼ系の活性化が重要である. 第68回日本血液学会総会.

8)小埜良一、北村俊雄、野阪哲哉（演者）. (2007年3月) MLL融合蛋白による多段階発癌におけるRaf-MAP キナーゼ系活性化の重要性. 日本プロテインホスファターゼ研究会 第3回国内集会.

H. 知的財産権の出願・登録状況

1. 特許取得

なし

2. 実用新案登録

なし

3. その他

なし

研究成果の刊行に関する一覧表

書籍

著者氏名	論文タイトル名	書籍全体の編集者氏名	書　籍　名	出版社名	出版地	出版年	ページ
該当なし							

雑誌

発表者氏名	論文タイトル名	発表誌名	巻号	ページ	出版年
川島　敏行	Rac1 and a GTPase activating protein MgcRacGAP are required for nuclear translocation of STAT transcription factors.	THE JOURNAL OF CELL BIOLOGY	175	937-946	2006
沖　俊彦	Integrin aIIbb3 induces the adhesion and activation of mast cells through interaction with fibrinogen.	THE JOURNAL OF IMMUNOLOGY	176	52-60	2006

Rac1 and a GTPase-activating protein, MgcRacGAP, are required for nuclear translocation of STAT transcription factors

Toshiyuki Kawashima,[1] Ying Chun Bao,[1] Yasushi Nomura,[1] Yuseok Moon,[1,4] Yukio Tonozuka,[1] Yukinori Minoshima,[1] Tomonori Hatori,[1] Akiho Tsuchiya,[1] Mari Kiyono,[2] Tetsuya Nosaka,[2] Hideaki Nakajima,[3] David A. Williams,[5] and Toshio Kitamura[1]

[1]Division of Cellular Therapy, [2]Division of Hematopoietic Factors, and [3]Center of Excellence, The Institute of Medical Science, University of Tokyo, Minato-ku, Tokyo 108-8639, Japan
[4]Department of Microbiology and Immunology, Medical Research Institute, Pusan National University Medical School, Busan 602-739, Korea
[5]Division of Experimental Hematology, Cincinnati Children's Hospital Medical Center, Cincinnati, OH 45229

STAT transcription factors are tyrosine phosphorylated upon cytokine stimulation and enter the nucleus to activate target genes. We show that Rac1 and a GTPase-activating protein, MgcRacGAP, bind directly to p-STAT5A and are required to promote its nuclear translocation. Using permeabilized cells, we find that nuclear translocation of purified p-STAT5A is dependent on the addition of GTP-bound Rac1, MgcRacGAP, importin α, and importin β. p-STAT3 also enters the nucleus via this transport machinery, and mutant STATs lacking the MgcRacGAP binding site do not enter the nucleus even after phosphorylation. We conclude that GTP-bound Rac1 and MgcRacGAP function as a nuclear transport chaperone for activated STATs.

Introduction

The signal transducer and activator of transcription (STAT) family consists of seven members (STAT1–4, -5A, -5B, and -6). STATs are phosphorylated by cytokine stimulation, form homo- or heterodimers, and enter the nucleus, where they regulate expression of their target genes (Darnell, 1996; Ihle, 1996). Although STATs have a variety of functions under physiological conditions, the pathological importance of STAT functions has also been reported in many studies. STAT3 and -5 were activated in a broad spectrum of human hematological malignancies as well as in solid tumors (Darnell, 2002). A constitutively active form of STAT5 and -3 transformed IL-3–dependent Ba/F3 cells and fibroblasts, respectively (Onishi et al., 1998; Bromberg et al., 1999; Nosaka et al., 1999). An internal tandem duplication (ITD) mutant of receptor tyrosine kinase Flt3 (ITD-Flt3), a causative mutation of acute myeloid leukemia (Yokota, et al., 1997; Hayakawa et al., 2000), induced phosphorylation of STAT5 on its tyrosine residues, thereby playing critical roles in cell transformation (Mizuki et al., 2000; Zhang et al., 2000; Murata et al., 2003).

The mechanisms by which STATs are phosphorylated by cytokines and the activated STATs regulate the expression of the target genes have been well characterized. How activated STATs are transported to the nucleus has also been investigated; activated STAT1 and -3 were reported to bind importin α5 and several importin αs, respectively, which mediated the nuclear transport of STATs (Sekimoto et al., 1997; McBride et al., 2002; Liu et al., 2005; Ushijima et al., 2005; Ma and Cao, 2006). However, molecules other than importins could also participate in the regulation of the nuclear translocation of STATs.

We have recently described the interactions among STAT3, Rac1, and a Rac/Cdc42 GTPase-activating protein (GAP), MgcRacGAP (male germ cell Rac-GAP), and have shown that MgcRacGAP is required for transcriptional activation of STAT3 (Tonozuka et al., 2004). However, the mechanisms by which Rac and MgcRacGAP regulate transcriptional activation of STAT3 remained unclear. In the present work, we investigated the molecular mechanisms of nuclear transport of a tyrosine-phosphorylated form of STAT5A, a close relative of STAT3, and found that GTP-bound Rac1 and MgcRacGAP were required for transport of activated STATs to the nucleus, indicating a novel function of Rac1 GTPase.

Correspondence to Toshio Kitamura: kitamura@ims.u-tokyo.ac.jp

Abbreviations used in this paper: DBD, DNA binding domain; EMSA, electrophoretic mobility shift analysis; GAP, GTPase-activating protein; ITD, internal tandem duplication; MBP, maltose binding protein; MgcRacGAP, male germ cell Rac-GAP; STAT, signal transducer and activator of transcription; TB, transport buffer.

The online version of this article contains supplemental material.

© The Rockefeller University Press $8.00
The Journal of Cell Biology, Vol. 175, No. 6, December 18, 2006 937–946
http://www.jcb.org/cgi/doi/10.1083/jcb.200604073

Supplemental Material can be found at:
http://www.jcb.org/cgi/content/full/jcb.200604073/DC1

Results

STAT5A, Rac, and MgcRacGAP form a complex in hematopoietic cells

To test whether Rac1 and MgcRacGAP bind STAT5A, as was the case for STAT3 (Tonozuka et al., 2004), we did coimmunoprecipitation. STAT5A and MgcRacGAP were coimmunoprecipitated with Rac1 (Fig. 1 A) and Rac2 in Ba/F3 cells (unpublished data). In addition, STAT5A was coimmunoprecipitated with MgcRacGAP in Ba/F3 cells and in several other human and mouse cell lines, as well as in human primary T cells (unpublished data). These data show that Rac, STAT5A, and MgcRacGAP form a complex in vivo.

Augmentation of MgcRacGAP association with STAT5A by IL-3 stimulation

A considerable amount of STAT5A protein was coimmunoprecipitated with MgcRacGAP in IL-3–starved Ba/F3 cells, and this association was enhanced by IL-3 stimulation (Fig. 1 B, left). Vice versa, a small amount of MgcRacGAP protein was coimmunoprecipitated with STAT5A in the starved cells, and this association was enhanced by IL-3 (Fig. 1 B, middle). In Ba/F3 cells expressing a constitutively active form of STAT5A (CA-STAT5A), which is more stable in the phosphorylated form than the wild-type STAT5A (Onishi et al., 1998), a considerable amount of STAT5A protein bound MgcRacGAP, even in unstimulated cells. This binding was also enhanced by IL-3 (Fig. 1 C). Thus, the association between MgcRacGAP and STAT5A does not require phosphorylation of STAT5A, but is enhanced by phosphorylation.

To map the interacting domains between MgcRacGAP and STAT5A, we prepared a series of truncated mutants of MgcRacGAP and STAT5A fused with maltose binding protein (MBP; Fig. S1, a, b, d, and e, available at http://www.jcb.org/cgi/content/full/jcb.200604073/DC1). It was found that STAT5A and Rac1 interacted with the Cys-rich and GAP domains of MgcRacGAP, whereas MgcRacGAP interacted with the DNA-binding domain (DBD) of STAT5A (Fig. S1, c and f). The binding domains between STAT5A and MgcRacGAP were similar to those between STAT3 and MgcRacGAP (Tonozuka et al., 2004).

Simultaneous translocation of STAT5A and MgcRacGAP to the nucleus upon IL-3 stimulation

We next investigated the stoichiometry of STAT5A/MgcRacGAP binding in the cytoplasm or nucleus. IL-3–starved Ba/F3 cells were stimulated with IL-3 for 0, 15, or 90 min, and the cell lysates were fractionated. The cytosol and nuclear fractions were then immunodepleted with the anti-MgcRacGAP or anti-STAT5A antibody. The amounts of total STAT5A and tyrosine-phosphorylated STAT5A (p-STAT5A) in the nuclear fraction increased 15 min after IL-3 stimulation and decreased 90 min after IL-3 stimulation (Fig. 2 A, a–d, lanes for the control antibody). Notably, most of p-STAT5A in the cytosolic fractions was immunodepleted with the anti-MgcRacGAP antibody as well as with the anti-STAT5A antibody (Fig. 2 A, c). On the other hand, a considerable part of p-STAT5A was left in the nuclear extracts of IL-3–stimulated cells after the immunodepletion with the anti-MgcRacGAP antibody

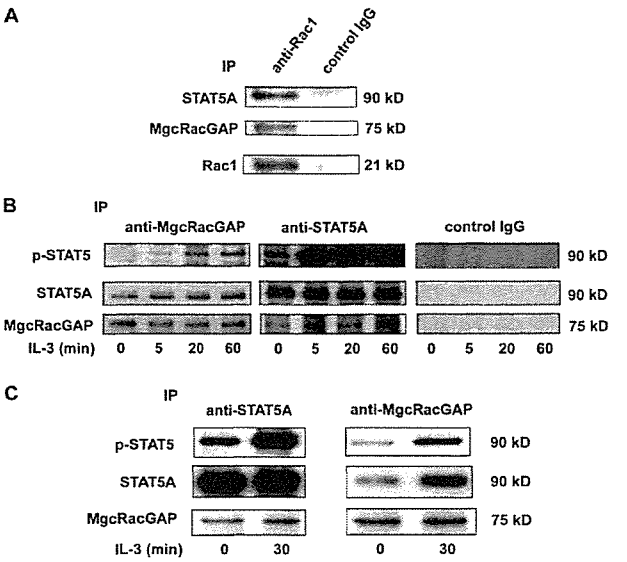

Figure 1. **MgcRacGAP, Rac1, and STAT5 formed a protein complex in IL-3–dependent Ba/F3 cells.** (A) STAT5A and MgcRacGAP were coprecipitated with Rac1. The cell lysates of IL-3–dependent Ba/F3 cells were subjected to immunoprecipitation with an anti-Rac1 or control antibody, followed by the immunoblotting with the anti-MgcRacGAP, anti-STAT5A, or anti-Rac1 antibody. (B) IL-3 enhanced association between STAT5A and MgcRacGAP. Ba/F3 cells were incubated in the presence or absence of 5 ng/ml IL-3 for the times indicated, and the cell lysates were subjected to immunoprecipitation with the anti-MgcRacGAP, anti-STAT5A, or control antibody, followed by the immunoblotting with the anti-p-STAT5 (top), anti-STAT5A (middle), or anti-MgcRacGAP antibody (bottom). Each row of images of the immunoprecipitation using the anti-MgcRacGAP and anti-STAT5A antibodies is derived from the same exposure of one gel, and each using the control antibody is derived from a similar exposure of the different gel. (C) The association of STAT5A and MgcRacGAP was enhanced in Ba/F3 cells expressing CA-STAT5A. Ba/F3 cells expressing CA-STAT5A were incubated in the presence or absence of 5 ng/ml IL-3 for 30 min, and cell lysates were subjected to immunoprecipitation with the anti-STAT5A (left) or anti-MgcRacGAP antibody (right), followed by the immunoblotting with the anti-p-STAT5 (top), anti-STAT5A (middle), or anti-MgcRacGAP antibody (bottom). Each row of images is derived from the same exposure of one gel.

(Fig. 2 A, a). These results suggested that most of p-STAT5A was bound by MgcRacGAP in the cytoplasm of IL-3–stimulated cells and was released from MgcRacGAP in the nucleus.

The amount of cytoplasmic STAT5A immunoprecipitated with the anti-MgcRacGAP antibody gradually increased after IL-3 stimulation (Fig. 2 A, h), and concomitantly the amount of cytoplasmic STAT5A immunodepleted with the anti-MgcRacGAP antibody gradually decreased (Fig. 2 A, d), implicating that MgcRacGAP maintained interaction with STAT5A in the cytoplasm of IL-3–stimulated cells even after the dephosphorylation of STAT5A. The fractionation was confirmed by Western blotting with the anti-HDAC (for nuclear fraction) or RhoA (for cytosol fraction) antibody (unpublished data).

Next, we visualized STAT5A and MgcRacGAP by immunostaining using adherent 293T cells. To enhance phosphorylation and nuclear translocation of STAT5, we used a constitutively active tyrosine kinase receptor, ITD-Flt3 (Yokota et al., 1997). In the absence of ITD-Flt3, ectopically expressed STAT5A-Flag localized to the cytoplasm and colocalized in part with the endogenous MgcRacGAP. Expression of ITD-Flt3 led to translocation

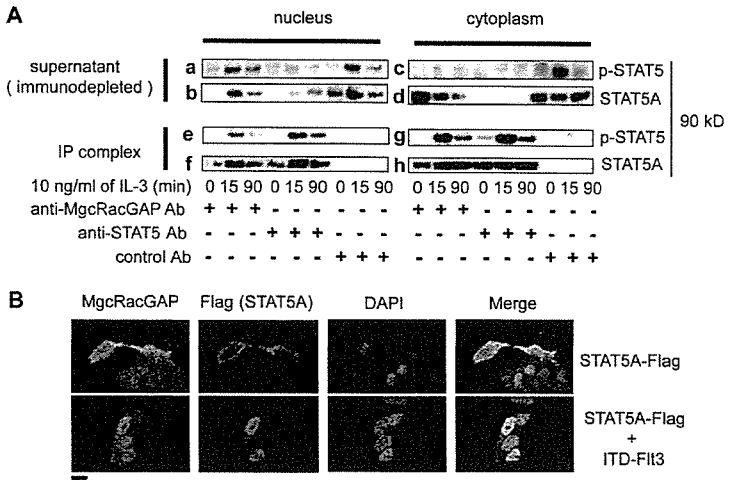

Figure 2. **STAT5A and MgcRacGAP simultaneously entered the nucleus.** (A) Stoichiometry of the association between MgcRacGAP and p-STAT5A or total STAT5A in the cytoplasm and nucleus. IL-3–starved Ba/F3 cells were stimulated with IL-3 for the times indicated, and cytosol and nuclear extracts were prepared as described previously (Nakamura et al., 2002). 10 μg of protein for each of the extracts was immunodepleted with the anti-MgcRacGAP, anti-STAT5A, or control antibody, followed by immunoblotting with the anti–p-STAT5 and anti-STAT5A antibodies (a–d). The immunoprecipitates were also examined by Western blotting with the anti–p-STAT5 and anti-STAT5 antibodies (e–h). (B) STAT5A and MgcRacGAP translocated into the nucleus upon ITD-Flt3 stimulation in 293T cells. Cells were transfected with pME/STAT5A-Flag together with pMKIT (MOCK; top) or pMKIT/ITD-Flt3 (bottom). After 36 h, cells were immunostained with the anti-MgcRacGAP and anti-Flag antibodies and viewed using a Fluoview FV300 confocal microscope. Bar, 10 μm.

and colocalization of STAT5A and MgcRacGAP in the nucleus (Fig. 2 B). These results indicated that MgcRacGAP translocated to the nucleus concurrently with STAT5A in response to IL-3 and ITD-Flt3 stimulation. Intriguingly, a dominant-negative form of Rac1, N17Rac1, completely inhibited the ITD-Flt3–induced nuclear translocation of STAT5A (Fig. S2, available at http://www.jcb.org/cgi/content/full/jcb.200604073/DC1). This result suggested that the GTP-bound form of Rac1 was required for the nuclear accumulation of activated STAT5A. However, N17Rac1 was recently reported to inhibit not only Rac1 but also other Rho-GTPases (Debreceni et al., 2004). To confirm that the N17Rac1 inhibition of nuclear translocation of p-STAT5A was indeed due to the inhibition of Rac1, we used mouse embryonic fibroblasts derived from gene-targeted conditional Rac1-flox mice in the Rac2-null background (Gu et al., 2003).

Rac1 is required for the nuclear translocation of p-STAT5A in mouse embryonic fibroblast cells

ITD-Flt3 induced the nuclear localization of STAT5A-Flag in the presence of Rac1 (Fig. 3 A, a and b). However, when Rac1 was depleted by Cre recombinase in $Rac2^{-/-}Rac1^{flox/flox}$ fibroblasts (Fig. 3 B), the nuclear translocation of STAT5A was severely impaired (Fig. 3 A, c and d), and even p-STAT5 mostly remained in the cytoplasm (Fig. 3 A, e and f). In addition, CA-STAT5A did not enter the nucleus in the absence of Rac1 (unpublished data). We performed a similar analysis using $Rac1^{flox/flox}Rac2^{wt/wt}$ fibroblasts and obtained identical results. These results demonstrate that Rac1 plays an essential role in the nuclear translocation of p-STAT5A.

Rac1 and MgcRacGAP were required for the nuclear accumulation and transcriptional activation of STAT5A

We next used siRNA to knock down Rac1 or MgcRacGAP expression in Ba/F3 cells where STAT5 activation is required for cell growth. The siRNA treatment for Rac1 or MgcRacGAP resulted in severe growth retardation of Ba/F3 cells and caused apoptosis in some cells. The total cell number was only one tenth or one fifth 48 h after siRNA treatment for Rac1 or MgcRacGAP, respectively (unpublished data). The siRNA treatment for MgcRacGAP led to the formation of multinucleated cells, as reported previously (Mishima et al., 2002), but no more than 20% of the cells, indicating the failure of cytokinesis by MgcRacGAP depletion is not the major cause of the growth inhibition.

We then did semiquantitative RT-PCR analysis to test whether transcriptional activation of STAT5 is affected by the knock down of Rac1 or MgcRacGAP and found that expression of bcl-xL, one of the STAT5 target genes, was severely impaired by the siRNA treatment (Fig. 4 A). We also confirmed that siRNA treatments specifically decreased the expression levels of Rac1 or MgcRacGAP protein but not those of RhoA and HDAC, similar to the results shown in Fig. 4 B (not depicted).

We also investigated whether knock down of Rac1 or MgcRacGAP affects the subcellular distribution of STAT5A and p-STAT5A in Ba/F3 cells before and after IL-3 stimulation. The siRNA-treated Ba/F3 cells were starved for 6 h after the isolation of live cells using Ficoll and stimulated with IL-3 (15 min), and the cell lysates were fractionated. The siRNA treatments specifically decreased expression levels of Rac1 or MgcRacGAP protein (Fig. 4 B, c and d) but not those of RhoA and HDAC (Fig. 4 B, e and f). The IL-3–induced nuclear accumulation of STAT5A and p-STAT5A was almost completely blocked in Ba/F3 cells treated with either Rac1 or MgcRacGAP siRNA when compared with those treated with the control siRNA (Fig. 4 B, a and b). The same treatment moderately decreased the amounts of p-STAT5A and total STAT5A in the cytoplasmic fraction (Fig. 4 B, a and b), suggesting that Rac1 and MgcRacGAP enhance the IL-3–induced phosphorylation of STAT5A and somehow stabilize STAT5A in the cytoplasm.

Direct interaction between STATs and MgcRacGAP/Rac1 regulates the activation of STATs through facilitating their tyrosine phosphorylation and nuclear translocation

We previously found that STAT3 bound MgcRacGAP through its DBD (Tonozuka et al., 2004). To examine whether MgcRacGAP regulated transcriptional activity of STAT3 and -5A through direct interaction, we attempted to produce mutant STATs lacking

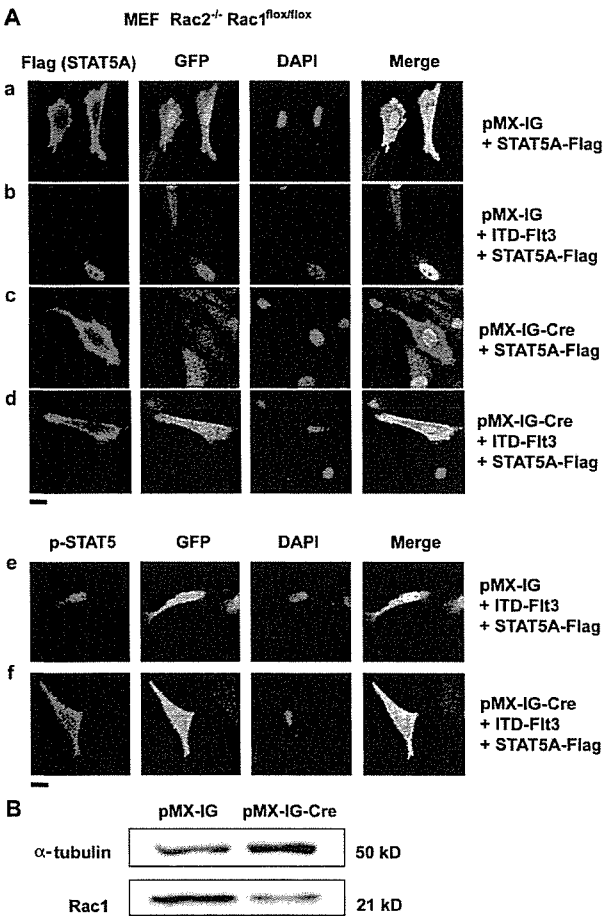

Figure 3. **The nuclear translocation of p-STAT5 was not observed in the Rac1-knockout mouse embryonic fibroblasts.** (A) The nuclear translocation of ITD-Flt3–induced p-STAT5 was impaired in the $Rac2^{-/-}Rac1^{flox/flox}$ fibroblasts. The $Rac2^{-/-}Rac1^{flox/flox}$ fibroblasts were transduced with a control pMX-IG (a and b) or pMX-IG-Cre (c and d) retrovirus vector. After 3 d, cells were transiently cotransfected with pME/STAT5A-Flag and MOCK (a and c) or pMKIT/ITD-Flt3 (b and d). After 36 h, the cells were fixed and immunostained with the anti-Flag antibody (a–d, left) or anti–p-STAT5 antibody (e and f, left). Bars, 10 μm. (B) Expression of Rac1 was depleted in the $Rac2^{-/-}Rac1^{flox/flox}$ fibroblasts by Cre recombinase. Expression of α-tubulin and Rac1 was examined in the $Rac2^{-/-}Rac1^{flox/flox}$ fibroblasts retovirally transduced with a control pMX-IG or pMX-IG-Cre.

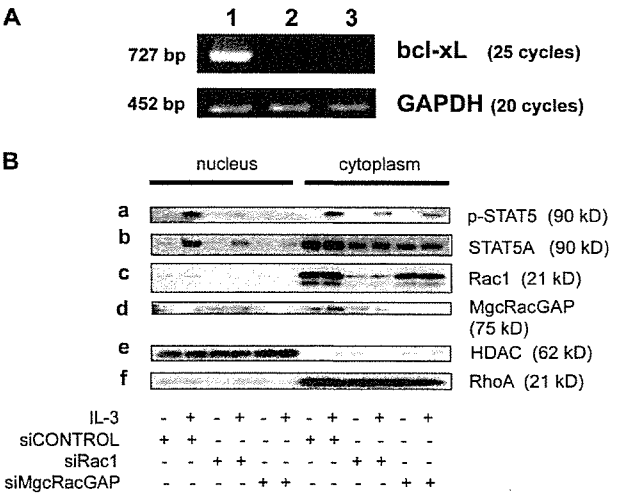

Figure 4. **Rac1 and MgcRacGAP were required for IL-3–induced nuclear accumulation and transcriptional activation of p-STAT5A.** (A) IL-3–induced transcriptional activation of STAT5A was suppressed by knock down of Rac1 or MgcRacGAP. Expression of bcl-xL or GAPDH mRNA was examined in Ba/F3 cells treated with the control siRNA (lane 1), Rac1 siRNA (lane 2), or MgcRacGAP siRNA (lane 3). 24 h after the siRNA treatment, the live cells were collected using Ficoll and subjected to semiquantitative RT-PCR. (B) IL-3–induced nuclear accumulation of p-STAT5A was impaired by knock down of Rac1 or MgcRacGAP. The intracellular distribution of p-STAT5A or total STAT5A in the IL-3–stimulated or unstimulated Ba/F3 cells pretreated with the control, Rac1, or MgcRacGAP siRNA (a and b). Note that Rac1 or MgcRacGAP expression was specifically suppressed by siRNA (c and d). Cytosol and nuclear extracts were prepared as described previously (Nakamura et al., 2002) and validated by Western blot using an anti-HDAC antibody or anti-RhoA antibody (e and f).

the MgcRacGAP binding site. To this end, we narrowed down the binding site in DBD-STAT3 to a 25-amino-acid stretch, using MBP-fused DBD-STAT3 truncations (DB1-DB6; Fig. S3 A, available at http://www.jcb.org/cgi/content/full/jcb.200604073/DC1). We found that only DB2 (aa 338–362) of DBD-STAT3 interacted with MgcRacGAP (Fig. S3 B). Conversely, the mutant of DBD-STAT3 lacking DB2 (DBD-STAT3-dDB2) did not bind MgcRacGAP (Fig. S3 C). These results clearly demonstrated that the DB2 region (25 amino acid) of STAT3 bound MgcRacGAP. This region is well conserved among STAT family proteins and harbors a β-sheet structure, which is thought to mediate protein–protein interaction. Purified MgcRacGAP was pulled down by the MBP-DB2 of STAT3, and the corresponding region of STAT5 (aa 341–365) fused with MBP but not by MBP alone, demonstrating that MgcRacGAP directly bound DB2 of STAT3 and -5 (Fig. S3 D and Fig. 5 A). Both of the STAT3 and -5A mutants lacking DB2 (STAT3- and STAT5A-dDB2) did not bind MgcRacGAP and the extent of tyrosine phosphorylation of these mutants was less prominent after IL-6 or ITD-Flt3 stimulation (Fig. 5 B and not depicted). In addition, STAT3- and STAT5A-dDB2 lacked their transcriptional activities (Fig. S3 E and Fig. 5 C). These results indicated that the interaction of MgcRacGAP/Rac1 with STAT3 and -5A facilitates cytokine receptor–induced tyrosine phosphorylation of both STAT3 and -5A. Considerable decrease in the tyrosine phosphorylation of STAT5A was also observed when Rac1 or MgcRacGAP was knocked down (Fig. 4 B, a). Intriguingly, MgcRacGAP also interacted with JAK2 (Fig. 5 D), suggesting that MgcRacGAP/Rac1 also mediated the tyrosine phosphorylation of STATs through the interaction with JAK2. Importantly, STAT3- and STAT5A-dDB2 that do not bind MgcRacGAP did not enter the nucleus even after tyrosine phosphorylation by IL-6 or ITD-Flt3 (Fig. 5 E and not depicted), suggesting that MgcRacGAP/Rac1 is required not only for nuclear translocation of p-STATs but also for efficient tyrosine phosphorylation of STATs.

MgcRacGAP and GTP-bound Rac1 were required for the nuclear translocation of p-STAT5A in cytosol-free digitonin-permeabilized cells

We established a nuclear transport assay using semi-intact permeabilized cells (Adam et al., 1990), which enables us to

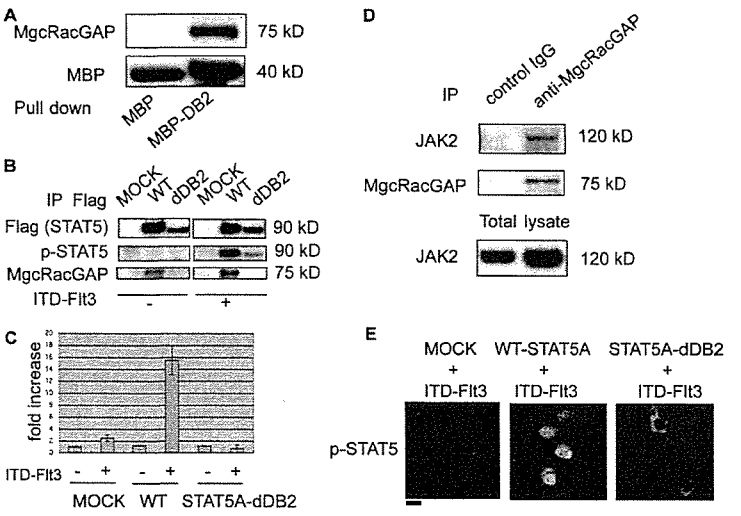

Figure 5. **The mutant of STAT5A, which lacks MgcRacGAP binding site, was not efficiently tyrosine phosphorylated by ITD-Flt3 stimulation and did not enter the nucleus even after tyrosine phosphorylation.** (A) The DB2 region of STAT5 directly interacted with MgcRacGAP in vitro. Full-length MgcRacGAP was expressed in Sf-9 cells using the baculovirus vector and was purified from infected Sf-9 cells. The recombinant MgcRacGAP was pulled down by MBP-DB2 or MBP-bound beads and subjected to Western blot analysis with the anti-MgcRacGAP (top) or anti-MBP antibody for the loading control (bottom). (B) The deletion mutant of DB2 did not bind MgcRacGAP, and the STAT5 phosphorylation was considerably impaired by the deletion of DB2. Expression and tyrosine phosphorylation of Flag-tagged STAT5A-dDB2 (top and middle, respectively) were examined in the MOCK or ITD-Flt3–transfected 293T cells. The interactions of MgcRacGAP with the WT-STAT5A or STAT5A-dDB2 were also examined in the MOCK or ITD-Flt3–transfected 293T cells (bottom). Images of the immunoblots using the MOCK or ITD-Flt3–transfected cells are derived from the same exposure of one gel that was cut to remove intervening lanes. (C) The transcriptional activity of STAT5-dDB2 was impaired. Luciferase activities were examined in the lysates of ITD-Flt3–stimulated 293T cells cotransfected with the STAT5-reporter plasmid together with internal control reporter plasmids and the MOCK vector (pME), the expression vector for the Flag-tagged WT-STAT5, or STAT5-dDB2 mutant. The results shown are the mean ± SD of three independent experiments. (D) MgcRacGAP was coprecipitated with JAK2. The cell lysates of 293T cells transfected with the expression vector (pRK5) for JAK2 were subjected to immunoprecipitation with the anti-MgcRacGAP or control antibody, followed by the immunoblotting with the anti-JAK2 (top) or anti-MgcRacGAP antibody (middle). Levels of transfected JAK2 were assayed by blotting with the anti-JAK2 antibody (bottom). (E) STAT5A-dDB2 did not enter the nucleus even after the phosphorylation. The 293T cells were cotransfected with pMKIT/ITD-Flt3 together with the MOCK (left), the expression vector for the Flag-tagged WT-STAT5A (middle), or STAT5A-dDB2 (right). After 24 h, the cells were fixed and immunostained with the anti–p-STAT5 antibody. Bar, 10 μm.

biochemically analyze the roles of Rac1 and MgcRacGAP in the nuclear import of p-STAT5A. We confirmed the purities of STAT5A, MgcRacGAP, V12Rac1, N17Rac1, importin α1, importin α5, importin β1, Ran, and NTF2 produced by Sf-9 cells, and the tyrosine phosphorylation of STAT5A induced by coexpression with the kinase domain of JAK2 in Sf-9 cells (Fig. 6, A and B). It was confirmed that the purified p-STAT5A bound DNA in electrophoretic mobility shift analysis (EMSA) in a similar fashion with GM-CSF–activated STAT5 in TF-1 cells (Fig. S4 A, available at http://www.jcb.org/cgi/content/full/jcb.200604073/DC1), indicating that the recombinant in vivo phosphorylated STAT5A formed a proper dimer. Permeabilized HeLa cells were incubated with the indicated combinations of purified proteins in transport buffer (TB) plus an energy regenerating system. After the import reaction in the cells incubated with purified unphosphorylated STAT5A, a considerable amount of unphosphorylated STAT5A was detected at the cytoplasm in most cells (Fig. 6 C, a). The addition of purified MgcRacGAP, V12Rac1, importin α1, and importin β1 did not affect localization of unphosphorylated STAT5A (Fig. 6 C, b–d and f). Although rabbit reticulocyte lysate reduced cytoplasmic localization of unphosphorylated STAT5A (Fig. 6 C, e), it induced both the nuclear and plasma membrane localization of p-STAT5A (Fig. 6 C, k). These results suggested that rabbit reticulocyte lysate contained cofactors that are required for the nuclear translocation of p-STAT5A in this transport assay. Interestingly, p-STAT5A accumulated at the nuclear membrane, with some migrating into the nucleus in the presence of purified MgcRacGAP and V12Rac1, but the nuclear translocation of p-STAT5A was inhibited in the presence of purified MgcRacGAP and N17Rac1 (Fig. 6 C, h and i). These results indicate that the GTP-bound form of Rac1 and MgcRacGAP facilitate the nuclear translocation of p-STAT5A. Given that purified importin β1 also accumulated mostly in the nuclear envelope and only partially migrated to the nucleus in our assay system (unpublished data) as reported previously (Kutay et al., 1997), the accumulation of p-STAT5 and importin β1 in the nucleus might have been caused by residual amounts of nuclear transporters left in the assay system. Thus, it is likely that the GTP-bound form of Rac1 and MgcRacGAP play critical roles in targeting p-STAT5A to the nuclear envelope and that cofactors are required for the efficient nuclear import of p-STAT5A from the nuclear envelope. In fact, nuclear translocation of p-STAT5A was enhanced by further addition of the purified nuclear transporters, including importin α1, importin β1, Ran, and NTF2 to the assay (Fig. 6 C, j). This nuclear translocation of p-STAT5A was not observed in the absence of MgcRacGAP even in the presence of cofactors (Fig. 6 C, l).

To confirm whether the unphosphorylated recombinant STAT5A conserved a native folded state, we did nuclear transport assay using the in vitro phosphorylated STAT5A. The recombinant full-length JAK2 efficiently phosphorylated the recombinant STAT5A in the kinase reaction buffer (Fig. S4 B). This in vitro phosphorylated STAT5A behaved in the nuclear transport assay like the in vivo phosphorylated STAT5A (Fig. S5, a–i, available at http://www.jcb.org/cgi/content/full/jcb.200604073/DC1). The nuclear transport of p-STAT5A requires both MgcRacGAP and V12Rac1. The nuclear import of the in vitro phosphorylated recombinant STAT5A was also achieved by the presence of the cytosol fraction of HeLa cells (HeLa-CS), which had been prepared as described previously (Adam et al., 1990). In addition, immunodepletion of MgcRacGAP or Rac1 considerably inhibited the nuclear import of the in vitro phosphorylated recombinant STAT5A (Fig. S5, j–m). This inhibition

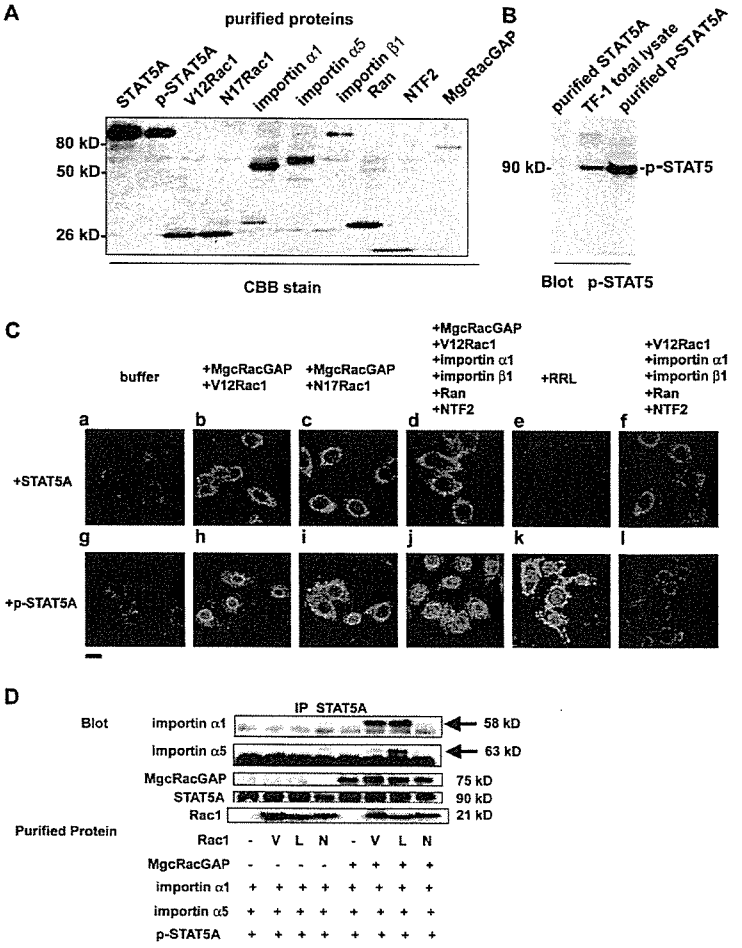

Figure 6. **Purified p-STAT5A accumulated to the nuclear envelope in the presence of V12Rac1 and MgcRacGAP in the nuclear transport assay.** (A) Coomassie blue (CBB) staining of purified STAT5A, p-STAT5A, V12Rac1, N17Rac1, importin α1, importin α5, importin β1, Ran, NTF2, or MgcRacGAP. (B) Western blot analysis of the STAT5A-Flag protein purified from Sf-9 cells with or without coexpression with the kinase domain of JAK using the anti–p-STAT5 antibody. Total cell lysate of GM-CSF–stimulated TF-1 was used as a control. (C) The nuclear transport assay. HeLa cells were permeabilized with 40 μg/ml digitonin. Incubation with 50 μl import mix was done at 37°C for 30 min. Import mix contained TB, an energy regenerating system, and a single or combinations of the following purified proteins as indicated: 1 μM STAT5A, p-STAT5A, V12Rac1, N17Rac1, MgcRacGAP, importin α1, importin β1, Ran, or NTF2. After the import reaction, the cells were fixed. STAT5A protein was detected using the anti-STAT5A antibody. Cells were examined using a Fluoview FV300 confocal microscope. A representative result of three independent experiments is shown. Bar, 10 μm. (D) The direct bindings of both GTP-bound Rac1 and MgcRacGAP facilitated the interaction of p-STAT5A with importin αs. Purified p-STAT5A was incubated with importin αs in the absence or presence of the indicated combinations of V12Rac1, L61Rac1, N17Rac1, or MgcRacGAP in TB containing 5% BSA to block nonspecific bindings. 1 μg of each purified protein was used for each sample. After the incubation for 30 min at RT, STAT5A was immunoprecipitated with anti-STAT5A antibody and washed three times with TB. The immunoprecipitates were subjected to Western blot analysis with the anti–importin α1, anti–importin α5, anti-Rac1, anti-MgcRacGAP, or anti-STAT5A antibody.

was restored by add-back of the purified recombinant MgcRacGAP or Rac1 (Fig. S5, n and o).

To determine whether the Rac1 activation or the presence of MgcRacGAP is required for the interaction of p-STAT5A with importin αs, an in vitro binding assay was done using purified proteins. Intriguingly, p-STAT5A formed complexes with importin α1 and α5 only in the presence of both MgcRacGAP and V12Rac1 or another constitutively active mutant L61Rac1, but not N17Rac1 (Fig. 6 D). These results demonstrated that GTP-bound Rac1 and MgcRacGAP functions as p-STAT5A nuclear chaperone, facilitating p-STAT5A to form protein complexes with importin αs.

Discussion

In the present work, we demonstrate that Rac1 and MgcRacGAP are essential for the nuclear translocation of STAT5A, based on the following observations. First, Rac1 and MgcRacGAP directly bound STAT5A, and the interaction between MgcRacGAP and STAT5A was enhanced by IL-3 stimulation. Second, STAT5A and MgcRacGAP simultaneously entered the nucleus upon IL-3 and ITD-Flt3 stimulation. Third, knock down of Rac1 or MgcRacGAP profoundly inhibited both the IL-3–induced transcriptional activation of STAT5A and the nuclear accumulation of p-STAT5A in IL-3–dependent Ba/F3 cells. Fourth, depletion of Rac1 in fibroblasts, as well as expression of N17Rac1 in 293T cells, prevented p-STAT5A from entering the nucleus. Fifth, p-STAT5A lacking the MgcRacGAP binding site (p-STAT5A–dDB2) did not accumulate in the nucleus. Last, in a nuclear transport assay, purified V12Rac1 and MgcRacGAP induced accumulation of purified p-STAT5A on the nuclear envelope, with some p-STAT5A migrating into the nucleus, and the further addition of nuclear transporters, including importin α1, importin β1, Ran, and NTF2, achieved the efficient nuclear translocation of p-STAT5A. Moreover, either the absence of MgcRacGAP or the presence of N17Rac1 inhibited this nuclear translocation of p-STAT5A.

Simon et al. (2000) suggested that an active form but not an inactive form of Rac1 bound STAT3 and played important roles in EGF-induced STAT3 activation. These authors did not, however, specifically examine the nuclear transport of STAT3. Interestingly, EGF receptor–mediated endocytosis is required for cytoplasmic transport of STAT3 (Bild et al., 2002), and MgcRacGAP is recruited to the EGF receptor complex after EGF stimulation (Blagoev et al., 2003). We also found that STAT3 bound Rac1 and Rac2, which was enhanced by IL-6 stimulation.

In addition, STAT3 bound MgcRacGAP, which was required for the transcriptional activation of STAT3, and some population of MgcRacGAP entered the nucleus together with STAT3 (Tonozuka et al., 2004). Although these results suggested a role of Rac1/MgcRacGAP in STAT3 activation, the underlying molecular mechanisms remained elusive. We studied the functional interactions using a nuclear transport assay and found that the nuclear translocation of p-STAT3 as well as p-STAT5A was induced in the presence of a combination of purified proteins, including V12Rac1, MgcRacGAP, importin α1, importin β1, Ran, and NTF2 (Fig. 6, Fig. S5, and not depicted). These results demonstrate a novel Rac1 function in the nuclear transport of p-STAT3 as well as p-STAT5A.

Although we showed the results for STAT5A, we obtained identical results in experiments so far performed for closely related STAT5B (unpublished data). In addition, the phenotypes of STAT3- and STAT5A-dDB2 were nearly identical (Fig. 5 and Fig. S3), and the region of STAT3 that binds to MgcRacGAP (STAT3-DBD-DB2) is well conserved among STAT family proteins, suggesting a general role for MgcRacGAP and Rac1 in the nuclear transport of p-STAT proteins.

Involvement of Rac1 in the nuclear transport of STATs

The Rho family small GTPases play key roles in a variety of cellular functions, including regulation of cell cycle, transcription, and transformation (Bishop and Hall, 2000). Among them, the Rac subfamily consists of three known members: Rac1, Rac2, and Rac3. Although Rac1 and Rac3 are ubiquitously expressed, Rac2 expression is specific in hematopietic cells. Rac1 and Rac2 were implicated in both distinct and overlapping functions, including cell migration, membrane ruffling, production of superoxide, and phagocytosis (Ridley, 1995; Roberts et al., 1999; Bishop and Hall, 2000; Williams et al., 2000; Gu et al., 2003; Cancelas et al., 2005). Interestingly, the C-terminal region of Rac1 but not Rac2 or Rac3 contained a functional NLS, suggesting a role for Rac1 in the nucleus. Consistent with this, Rac1 was reported to play a role in the nuclear import of SmgGDS and p120 catenin (Lanning et al., 2003), members of the importin α–like armadillo family of proteins (Peifer et al., 1994; Chook and Blobel, 2001). In the present paper, using Rac1-deficient mouse embryonic fibroblasts, we demonstrate that Rac1 was critically required for the nuclear transport of p-STAT5A (Fig. 3).

Requirement of cofactors involved in importin α/β pathway for nuclear import of STAT5

It was reported that unphosphorylated STATs shuttled between the cytoplasm and nucleus (Zeng et al., 2002; Marg et al., 2004). Activated STAT1 was reported to bind importin α5, leading to its nuclear translocation (Sekimoto et al., 1997; McBride et al., 2002). How activated STAT3 is imported to the nucleus has remained controversial. Ushijima et al. (2005) showed that activated STAT3 binds importin α1, α3, and α5, and Ma and Cao (2006) demonstrated that activated STAT3 binds importin α5 and α7 but not α1, α3, or α4, whereas Liu et al. (2005) reported that STAT3 nuclear import is independent of tyrosine phosphorylation and mediated by importin α3. On the other hand, how activated STAT5A is imported to the nucleus remained largely elusive. It was reported that the ERBB4/HER4 receptor tyrosine kinase, which harbors the NLS sequence, functions as a STAT5A nuclear chaperone, implicating the NLS of STAT5A-associated molecules in the nuclear translocation of STAT5A (Williams et al., 2004). However, unlike ERBB4/HER4, ITD-Flt3 does not harbor an NLS and did not enter the nucleus (unpublished data). In the nuclear transport assay, most p-STAT5A accumulated to the nuclear envelope in the presence of V12Rac1 and MgcRacGAP, and further addition of the purified nuclear transporters, including importin α1, importin β1, Ran, and NTF2, facilitated the nuclear translocation of p-STAT5A (Fig. 6 C, j). Together, it is likely that the complex of p-STAT5, GTP-bound Rac1, and MgcRacGAP translocates to the nuclear envelope, where it recruits other factors such as importin α/β to pass through the nuclear pore complex into the nucleus. Indeed, direct interaction of both GTP-bound Rac1 and MgcRacGAP facilitated the interaction of p-STAT5A with importin αs (Fig. 6 D). In agreement with this, Rac1 harbors an NLS (Lanning et al., 2003) and MgcRacGAP harbors a bipartite NLS and binds importin αs (unpublished data). Interestingly, a mutant of MgcRacGAP lacking NLS strongly blocked the nuclear translocation of p-STATs in the nuclear transport assay even with V12Rac1, importin α1, importin β1, Ran, and NTF2 (unpublished data), suggesting a role of MgcRacGAP as an NLS-containing nuclear chaperone of p-STATs. Establishment of the nuclear transport assay for p-STATs has enabled us to clearly demonstrate the requirement of Rac1 and MgcRacGAP for the nuclear translocation of p-STATs.

The activities of small GTPases are regulated by two classes of proteins, GAPs and GEFs (guanine nucleotide exchange factors). In this paper, we did not address GEFs, but some, such as smgGDS or ECT-2, may also participate in the nuclear transport of STAT proteins. Based on the results that p-STAT5A binds importin αs only in the presence of MgcRacGAP and active forms of Rac1 but not inactive form of Rac1, we speculate that Rac1 inactivation by MgcRacGAP release p-STATs from the importin complex in the nucleus. To prove this hypothesis and clarify its molecular mechanisms, further work will be required.

Coordinate control of cell division and transcription

Another interesting question raised by our work concerns the coordinate control of cell division and transcription. We originally identified MgcRacGAP as a GAP protein that regulates IL-6–induced macrophage differentiation of leukemic M1 cells (Kawashima et al., 2000). Later, we and others found that MgcRacGAP or Cyk-4, an orthologue in *Caenorhabditis elegans*, played essential roles in cytokinesis (Jantsch-Plunger et al., 2000; Hirose et al., 2001; Van de Putte et al., 2001; Mishima et al., 2002). We further demonstrated that MgcRacGAP was phosphorylated at Serine 387 by Aurora-B at the midbody, functionally converted from Rac/Cdc42-GAP to Rho-GAP, and played essential roles to complete cell division in cytokinesis (Minoshima et al., 2003). In interphase, MgcRacGAP formed a

complex with Rac1 and STAT3 and was required for the full transcriptional activation of STAT3, thereby enhancing the differentiation of IL-6–stimulated M1 cells (Tonozuka et al., 2004). On the other hand, when STAT5 was activated by IL-3 or ITD-Flt3 in conjunction with Rac1 and MgcRacGAP, the cells proliferate. Thus, MgcRacGAP functions as a Rac-GAP to activate transcription of STAT in the nucleus of interphase cells, probably leading to cell proliferation or differentiation. At cytokinesis, it functions as a Rho-GAP to complete cytokinesis, indicating that the distinct roles of the Rho family small GTPases depend on the cell cycle.

Does Rac1 play a general role in nuclear transport of transcription-related proteins?

The experiments using N17Rac1 showed that Rac1 contributes to maximal activation of STAT1 and -3 in response to IFN-γ (Park et al., 2004). The molecular mechanisms of this phenomenon can be explained by our current results. Esufali and Bapat (2004) suggested that Rac1 plays some role in redistribution of β-catenin and that a mutant Rac1 lacking its NLS hampers nuclear localization of β-catenin, leading to attenuation of the β-catenin–dependent transcriptional activity of T cell factor/lymphoid enhancing factor. The authors stated that it was not yet clear whether the Rac1/β-catenin association facilitated nuclear import or retention of β-catenin or, alternatively, Rac1 augments the function of β-catenin as a coactivator. Given the results of the present study, however, it is likely that Rac1 also plays a critical role in the nuclear transport of β-catenin, suggesting a general role of Rac1 GTPase for the nuclear transport of transcription factors. It is tempting to speculate that Rac1 is a molecular link between changes in cytoskeletal organization and alterations in transcription.

Materials and methods

Culture, cytokines, and antibodies

Ba/F3 cells were maintained in RPMI1640 medium (Invitrogen) containing 10% FCS and 1 ng/ml mIL-3 (R&D Systems). An ecotropic retrovirus packaging cell line PLAT-E was maintained as described previously (Hirose et al., 2001). An anti-STAT5A antibody and anti-STAT5B antibody were obtained from R&D Systems. Affinity-purified anti-MgcRacGAP antibody was produced as described previously (Hirose et al., 2001). An anti-Rac1 mAb and anti–importin α1 mAb were purchased from BD Biosciences. The rabbit polyclonal anti-Rac1, anti-RhoA, anti-JAK2, and goat polyclonal anti-HDAC or anti–importin α5 antibodies were obtained from Santa Cruz Biotechnology, Inc.

Immunoprecipitation and Western blotting

Immunoprecipitation, gel electrophoresis, and immunoblotting were done as described previously (Kawashima et al., 2001), with minor modifications. Cell lysates (2×10^7 cells/ml) were incubated at 4°C for 2 h with the indicated antibodies and protein A–Sepharose. The immunoprecipitates were subjected to Western blot analysis with an anti–p-STAT5 mAb (Upstate Biotechnology), anti-MgcRacGAP, or anti-STAT5A antibody. The loading amounts were verified with the anti-STAT5A or anti-MgcRacGAP antibody after stripping the filters. The filter-bound antibody was detected using the ECL system (GE Healthcare). Cytosol and nuclear fractions were prepared as described previously (Nakamura et al., 2002).

MBP pull-down assays

MBP fusion proteins (0.5 μg) bound to amylose resin beads were incubated with cell lysates (10 μg) from IL-3–stimulated Ba/F3 cells as described previously (Tonozuka et al., 2004).

Transfection and immunostaining

The 293T cells were transfected with 1.0 μg pME/STAT5A-Flag together with 0.5 μg pMKIT (MOCK) or pMKIT/ITD-Flt3, and in some experiments cells were transfected with 0.5 μg pME/STAT5A-HA and 0.5 μg pMKIT (MOCK) or pMKIT/ITD-Flt3 together with 1.0 μg pCMV5/N17Rac1-Flag, using Lipofectamine Plus reagents (Life Technologies). After 24 h, cells were plated on glass coverslips, and the next day the cells were immunostained as described previously (Hirose et al., 2001).

Microscopy

Fluorescence images were analyzed on a confocal microscope (Fluoview FV300 Scanning Laser Biological Microscope IX 70 system; Olympus) equipped with two lasers (Ar 488 and HeNe 543) using a 60× oil objective (PlanApo; Olympus). Fluoview version 4.3 software (Olympus) was used for image acquisition from confocal microscopy. Photoshop 7.0 or Photoshop Elements 2.0 software (Adobe) was used for processing of images.

RNA interference and semiquantitative RT-PCR

For the silencing of Rac1 or MgcRacGAP, SMARTpool Rac1 or MgcRacGAP siRNA (L-041170 or L040081; Dharmacon) was used. A control siRNA was used as a nonsilencing control (Tonozuka et al., 2004). 5 μl of 40 μM double-stranded siRNA were introduced in to 2×10^6 cells of Ba/3F cells with Nucleofector II (Amaxa) set at program T-16 using a Cell Line Nucleofector kit V (Amaxa) according to the manufacturer's instruction. A control vector carrying GFP was introduced to >80% of Ba/3F cells under this condition. 24 h after transfection, live cells were isolated using Ficoll-Paque PLUS (GE Healthcare), and gene expression was examined by semiquantitative RT-PCR analysis as described previously (Nosaka et al., 1999). The primers used are as follows: 5′bcl-x, 5′-GAAAGAATTCACCATGTCTCAGAGCAACCGG-3′; 3′bcl-x, 5′-GAAAGCGGCCGCTCACTTCCGACTGAAGAGTG-3′; 5′GAPDH, 5′-ACCACAGTCCATGCCATCAC-3′; 3′GAPDH, 5′-TCCACCACCCTGTTGCTGTA-3′.

Production of retroviruses

High-titer retroviruses harboring Cre recombinase were produced in a transient retrovirus packaging cell line PLAT-E (Morita et al., 2000) and were used to deplete Rac1 in $Rac2^{-/-}$ $Rac1^{flox/flox}$ fibroblasts (Fig. 3 B).

Generation, expression, and purification of recombinant proteins in Sf-9 cells

To construct baculovirus vectors, the cDNAs encoding STAT5A, MgcRacGAP, V12Rac1, L61Rac1, N17Rac1, importin αs, importin β1, Ran, and NTF2 with the C-terminal Flag epitope tag, and a kinase domain of JAK2 (JH1; Saharinen et al., 2000) were subcloned into pBacPAK (BD Biosciences). The resulting constructs were used to obtain recombinant baculoviruses by cotransfection with Bsu36 I–digested BacPAK viral DNA (BD Biosciences) into Sf-9 cells according to the manufacturer's protocol. For protein expression, Sf-9 cells were infected with high-titer viral stocks for 96 h and lysed. The lysate was clarified by centrifugation, and the supernatant was immunoprecipitated with the anti-Flag M2-agarose affinity gel (Sigma-Aldrich) for 2 h at 4 °C. The recombinant Flag-tagged proteins were eluted with 3× Flag peptide (Sigma-Aldrich).

EMSA using purified p-STAT5A

To determine whether purified p-STAT5A formed a proper dimer, EMSA was performed using consensus sequence of STAT5A as a probe, as described previously (Kawashima et al., 2001).

In vitro kinase reaction

An in vitro kinase reaction of purified STAT5A was performed as described previously with minor modifications (Quelle et al., 1995). In vitro phosphorylated STAT5A was immunoprecipitated with the anti-Flag M2-agarose affinity gel and reeluted with a 3× Flag peptide. The purified in vitro phosphorylated STAT5A was dialyzed against TB, and the final concentrations of STAT5A protein were determined for use in SDS-PAGE and in the nuclear transport assay.

Preparation of fluorescent conjugates

FITC-labeled BSA (Sigma-Aldrich) conjugated with a synthetic peptide containing the SV40 large T antigen (CGGGPKKKRKVED; NLS-conjugated FITC-BSA) was prepared as described previously (Adam et al., 1990), as a control protein harboring an NLS. We confirmed that NLS-conjugated FITC-BSA was imported to the nucleus in our experimental conditions as reported previously (Kutay et al., 1997), which was not inhibited by immunodepletion of MgcRacGAP or Rac1 (Fig. S5, p–t).

Import assays with permeabilized cells

HeLa cells were grown on poly-L-lysine–coated coverslips and permeabilized with 40 μg/ml digitonin (Roche) in TB (20 mM Hepes, pH 7.3, 110 mM KOAC, 2 mM $Mg(OAC)_2$, 1 mM EGTA, 2 mM DTT, 0.4 mM PMSF, 3 μg/ml aprotinin, 2 μg/ml pepstatin A, 1 μg/ml leupeptin, and 20 mg/ml BSA) for 10 min at RT. Subsequently, the cells were washed twice in TB. Incubation with 50 μl import mix was performed at 37°C for 30 min. The import mix contained TB, an energy regenerating system (0.5 mM ATP, 0.5 mM GTP, 10 mM creatine phosphate, and 30 U/ml creatine phosphokinase), and 1 μM of purified unphosphorylated or phosphorylated STAT5A alone, or STAT5A plus the 1 μM of other purified cofactor proteins as indicated in Fig. 6 C. After the import reaction, the cells were washed with ice-cold TB and immunostained with the anti-STAT5A antibody and anti-p-STAT5 mAb as described previously (Hirose et al., 2001). Fixed cells were examined using a Fluoview FV300 confocal microscope (Olympus).

Online supplemental material

Fig. S1 depicts the binding domains of MgcRacGAP with STAT5A and that of STAT5A with MgcRacGAP. Fig. S2 shows that N17Rac1 expression inhibits the nuclear translocation of p-STAT5A. Fig. S3 shows that the DB2 region is required for the interaction of STAT3 with MgcRacGAP and the transcriptional activation of STAT3. Fig. S4 shows that purified p-STAT5A forms a dimer and binds DNA containing the STAT5 consensus sequence and that the purified STAT5A can be phosphorylated in vitro. Fig. S5 shows that the in vitro phosphorylated recombinant STAT5A can be imported to the nucleus in the nuclear transport assay and that immunodepletion of Rac1 or MgcRacGAP specifically inhibits the nuclear import of p-STAT5A using HeLa cytosol extract. Online supplemental material is available at http://www.jcb.org/cgi/content/full/jcb.200604073/DC1.

We thank Dr. Y. Kaziro for critical reading of the manuscript, Dr. T. Satoh for valuable discussions, and M. Ohara and Dovie Wylie for language assistance. We also thank R&D Systems for providing us with cytokines.

This work was supported by grants from the Ministry of Education, Science, Sports and Culture of Japan (16209 032) and a grant in aid from the Sumitomo Foundation. The Division of Hematopoietic Factors is supported by the Chugai Pharmaceutical Co., Ltd. David A. Williams was supported by grants from the National Institutes of Health (R01 DK62757).

Submitted: 13 April 2006
Accepted: 20 November 2006

References

Adam, S.A., R.S. Marr, and L. Gerace. 1990. Nuclear protein import in permeabilized mammalian cells requires soluble cytoplasmic factors. *J. Cell Biol.* 111:807–816.

Bild, A.H., J. Turkson, and R. Jove. 2002. Cytoplasmic transport of Stat3 by receptor-mediated endocytosis. *EMBO J.* 21:3255–3263.

Bishop, A.L., and A. Hall. 2000. Rho GTPases and their effector proteins. *Biochem. J.* 348:241–255.

Blagoev, B., I. Kratchmarova, S.E. Ong, M. Nielsen, L.J. Foster, and M. Mann. 2003. A proteomics strategy to elucidate functional protein-protein interactions applied to EGF signaling. *Nat. Biotechnol.* 21:315–318.

Bromberg, J.F., M.H. Wrzeszczynska, G. Devgan, Y. Zhao, R.G. Pestell, C. Albanese, and J.E. Darnell Jr. 1999. The JAK-STAT pathway: summary of initial studies and recent advances. Stat3 as an oncogene. *Cell.* 98:295–303.

Cancelas, J.A., A.W. Lee, R. Prabhakar, K.F. Stringer, Y. Zheng, and D.A. Williams. 2005. Rac GTPases differentially integrate signals regulating hematopoietic stem cell localization. *Nat. Med.* 11:886–891.

Chook, Y.M., and G. Blobel. 2001. Karyopherins and nuclear import. *Curr. Opin. Struct. Biol.* 11:703–715.

Darnell, J.E., Jr. 1996. The JAK-STAT pathway: summary of initial studies and recent advances. *Recent Prog. Horm. Res.* 51:391–403.

Darnell, J.E., Jr. 2002. Transcription factors as targets for cancer therapy. *Nat. Rev. Cancer.* 2:740–749.

Debreceni, B., Y. Gao, F. Guo, K. Zhu, B. Jia, and Y. Zheng. 2004. Mechanisms of guanine nucleotide exchange and Rac-mediated signaling revealed by a dominant negative trio mutant. *J. Biol. Chem.* 279:3777–3786.

Esufali, S., and B. Bapat. 2004. Cross-talk between Rac1 and dysregulated Wnt signaling pathway leads to cellular redistribution of β-catenin and TCF/LEF-mediated transcriptional activation. *Oncogene.* 23:8260–8271.

Gu, Y., M.D. Filippi, J.A. Cancelas, J.E. Siefring, E.P. Williams, A.C. Jasti, C.E. Harris, A.W. Lee, R. Prabhakar, S.J. Atkinson, et al. 2003. Hematopoietic cell regulation by Rac1 and Rac2 guanosine triphosphatases. *Science.* 302:445–449.

Hayakawa, F., M. Towatari, H. Kiyoi, M. Tanimoto, T. Kitamura, H. Saito, and T. Naoe. 2000. Tandem-duplicated Flt3 constitutively activates STAT5 and MAP kinase and introduces autonomous cell growth in IL-3-dependent cell lines. *Oncogene.* 19:624–631.

Hirose, K., T. Kawashima, I. Iwamoto, T. Nosaka, and T. Kitamura. 2001. MgcRacGAP is involved in cytokinesis through associating with mitotic spindle and midbody. *J. Biol. Chem.* 276:5821–5828.

Ihle, J.N. 1996. Janus kinases in cytokine signalling. *Philos. Trans. R. Soc. Lond. B Biol. Sci.* 351:159–166.

Jantsch-Plunger, V., P. Gonczy, A. Romano, H. Schnabel, D. Hamill, R. Schnabel, A.A. Hyman, and M. Glotzer. 2000. CYK-4: a Rho family GTPase activating protein (GAP) required for central spindle formation and cytokinesis. *J. Cell Biol.* 149:1391–1404.

Kawashima, T., K. Hirose, T. Satoh, A. Kaneko, Y. Ikeda, Y. Kaziro, T. Nosaka, and T. Kitamura. 2000. MgcRacGAP is involved in the control of growth and differentiation of hematopoietic cells. *Blood.* 96:2116–2124.

Kawashima, T., K. Murata, S. Akira, Y. Tonozuka, Y. Minoshima, S. Feng, H. Kumagai, H. Tsuruga, Y. Ikeda, S. Asano, et al. 2001. STAT5 induces macrophage differentiation of M1 leukemia cells through activation of IL-6 production mediated by NF-kappaB p65. *J. Immunol.* 167:3652–3660.

Kutay, U., E.I. Izaurralde, F.R. Bischoff, I.W. Mattaj, and D. Görlich. 1997. Dominant-negative mutants of importin-β block multiple pathways of import and export through the nuclear pore complex. *EMBO J.* 16:1153–1163.

Lanning, C.C., R. Ruiz-Velasco, and C.L. Williams. 2003. Novel mechanism of the co-regulation of nuclear transport of SmgGDS and Rac1. *J. Biol. Chem.* 278:12495–12506.

Liu, L., K.M. McBride, and N.C. Reich. 2005. STAT3 nuclear import is independent of tyrosine phosphorylation and mediated by importin-alpha3. *Proc. Natl. Acad. Sci. USA.* 102:8150–8155.

Ma, J., and X. Cao. 2006. Regulation of Stat3 nuclear import by importin alpha5 and importin alpha7 via two different functional sequence elements. *Cell. Signal.* 18:1117–1126.

Marg, A., Y. Shan, T. Meyer, T. Meissner, M. Brandenburg, and U. Vinkemeier. 2004. Nucleocytoplasmic shuttling by nucleoporins Nup153 and Nup214 and CRM1-dependent nuclear export control the subcellular distribution of latent Stat1. *J. Cell Biol.* 165:823–833.

McBride, K.M., G. Banninger, C. McDonald, and N.C. Reich. 2002. Regulated nuclear import of the STAT1 transcription factor by direct binding of importin-α. *EMBO J.* 21:1754–1763.

Minoshima, Y., T. Kawashima, K. Hirose, Y. Tonozuka, A. Kawajiri, Y.C. Bao, X. Deng, M. Tatsuka, S. Narumiya, W.S. May Jr., et al. 2003. Phosphorylation by aurora B converts MgcRacGAP to a RhoGAP during cytokinesis. *Dev. Cell.* 4:549–560.

Mishima, M., S. Kaitna, and M. Glotzer. 2002. Central spindle assembly and cytokinesis require a kinesin-like protein/RhoGAP complex with microtubule bundling activity. *Dev. Cell.* 2:41–54.

Mizuki, M., R. Fenski, H. Halfter, I. Matsumura, R. Schmidt, C. Muller, W. Gruning, K. Kratz-Albers, S. Serve, C. Steur, et al. 2000. Flt3 mutations from patients with acute myeloid leukemia induce transformation of 32D cells mediated by the Ras and STAT5 pathways. *Blood.* 96:3907–3914.

Morita, S., T. Kojima, and T. Kitamura. 2000. Plat-E: an efficient and stable system for transient packaging of retroviruses. *Gene Ther.* 7:1063–1066.

Murata, K., H. Kumagai, T. Kawashima, K. Tamitsu, M. Irie, H. Nakajima, S. Suzu, M. Shibuya, S. Kamihira, T. Nosaka, et al. 2003. Selective cytotoxic mechanism of GTP-14564, a novel tyrosine kinase inhibitor in leukemia cells expressing a constitutively active Fms-like tyrosine kinase 3 (FLT3). *J. Biol. Chem.* 278:32892–32898.

Nakamura, T., R. Ouchida, T. Kodama, T. Kawashima, Y. Makino, N. Yoshikawa, S. Watanabe, C. Morimoto, T. Kitamura, and H. Tanaka. 2002. Cytokine receptor common beta subunit-mediated STAT5 activation confers NF-kappa B activation in murine proB cell line Ba/F3 cells. *J. Biol. Chem.* 277:6254–6265.

Nosaka, T., T. Kawashima, K. Misawa, K. Ikuta, A.L. Mui, and T. Kitamura. 1999. STAT5 as a molecular regulator of proliferation, differentiation and apoptosis in hematopoietic cells. *EMBO J.* 18:4754–4765.

Onishi, M., T. Nosaka, K. Misawa, A.L. Mui, D. Gorman, M. McMahon, A. Miyajima, and T. Kitamura. 1998. Identification and characterization of a constitutively active STAT5 mutant that promotes cell proliferation. *Mol. Cell. Biol.* 18:3871–3879.

Park, E.J., K.A. Ji, S.B. Jeon, W.H. Choi, I.O. Han, H.J. You, J.H. Kim, I. Jou, and E.H. Joe. 2004. Rac1 contributes to maximal activation of STAT1 and STAT3 in IFN-gamma-stimulated rat astrocytes. *J. Immunol.* 173:5697–5703.

Peifer, M., S. Berg, and A.B. Reynolds. 1994. A repeating amino acid motif shared by proteins with diverse cellular roles. *Cell.* 76:789–791.

Quelle, F.W., W. Thierfelder, B.A. Witthuhn, B. Tang, S. Cohen, and J.N. Ihle. 1995. Phosphorylation and activation of the DNA binding activity of purified Stat1 by the Janus protein-tyrosine kinases and the epidermal growth factor receptor. *J. Biol. Chem.* 270:20775–20780.

Ridley, A.J. 1995. Rho-related proteins: actin cytoskeleton and cell cycle. *Curr. Opin. Genet. Dev.* 5:24–30.

Roberts, A.W., C. Kim, L. Zhen, J.B. Lowe, R. Kapur, B. Petryniak, A. Spaetti, J.D. Pollock, J.B. Borneo, G.B. Bradford, et al. 1999. Deficiency of the hematopoietic cell-specific Rho family GTPase Rac2 is characterized by abnormalities in neutrophil function and host defense. *Immunity.* 10:183–196.

Saharinen, P., K. Takaluoma, and O. Silvennoinen. 2000. Regulation of the Jak2 tyrosine kinase by its pseudokinase domain. *Mol. Cell. Biol.* 20:3387–3395.

Sekimoto, T., N. Imamoto, K. Nakajima, T. Hirano, and Y. Yoneda. 1997. Extracellular signal-dependent nuclear import of Stat1 is mediated by nuclear pore-targeting complex formation with NPI-1, but not Rch1. *EMBO J.* 16:7067–7077.

Simon, A.R., H.G. Vikis, S. Stewart, B.L. Fanburg, B.H. Cochran, and K. Guan. 2000. Regulation of STAT3 by direct binding to the Rac1 GTPase. *Science.* 290:144–147.

Tonozuka, Y., Y. Minoshima, Y.C. Bao, Y. Moon, Y. Tsubono, T. Hatori, H. Nakajima, T. Nosaka, T. Kawashima, and T. Kitamura. 2004. A GTPase activating protein binds STAT3 and is required for IL-6-induced STAT3 activation and for differentiation of a leukemic cell line. *Blood.* 104:3550–3557.

Ushijima, R., N. Sakaguchi, A. Kano, A. Maruyama, Y. Miyamoto, T. Sekimoto, Y. Yoneda, K. Ogino, and T. Tachibana. 2005. Extracellular signal-dependent nuclear import of STAT3 is mediated by various importin alphas. *Biochem. Biophys. Res. Commun.* 330:880–886.

Van de Putte, T., A. Zwijsen, O. Lonnoy, V. Rybin, M. Cozijnsen, A. Francis, V. Baekelandt, C.A. Kozak, M. Zerial, and D. Huylebroeck. 2001. Mice with a homozygous gene trap vector insertion in mgcRacGAP die during pre-implantation development. *Mech. Dev.* 102:33–44.

Williams, C.C., J.G. Allison, G.A. Vidal, M.E. Burow, B.S. Beckman, L. Marrero, and F.E. Jones. 2004. The ERBB4/HER4 receptor tyrosine kinase regulates gene expression by functioning as a STAT5A nuclear chaperone. *J. Cell Biol.* 167:469–478.

Williams, D.A., W. Tao, F. Yang, C. Kim, Y. Gu, P. Mansfield, J.E. Levine, B. Petryniak, C.W. Derrow, C. Harris, et al. 2000. Dominant negative mutation of the hematopoietic-specific Rho GTPase, Rac2, is associated with a human phagocyte immunodeficiency. *Blood.* 96:1646–1654.

Yokota, S., H. Kiyoi, M. Nakao, T. Iwai, S. Misawa, T. Okuda, Y. Sonoda, T. Abe, K. Kahsima, Y. Matsuo, and T. Naoe. 1997. Internal tandem duplication of the FLT3 gene is preferentially seen in acute myeloid leukemia and myelodysplastic syndrome among various hematological malignancies. A study on a large series of patients and cell lines. *Leukemia.* 11:1605–1609.

Zeng, R., Y. Aoki, M. Yoshida, K. Arai, and S. Watanabe. 2002. Stat5B shuttles between cytoplasm and nucleus in a cytokine-dependent and -independent manner. *J. Immunol.* 168:4567–4575.

Zhang, S., S. Fukuda, Y. Lee, G. Hangoc, S. Cooper, R. Spolski, W.J. Leonard, and H.E. Broxmeyer. 2000. Essential role of signal transducer and activator of transcription (Stat)5a but not Stat5b for Flt3-dependent signaling. *J. Exp. Med.* 192:719–728.

Integrin $\alpha_{IIb}\beta_3$ Induces the Adhesion and Activation of Mast Cells through Interaction with Fibrinogen[1]

Toshihiko Oki,* Jiro Kitaura,* Koji Eto,† Yang Lu,* Mari Maeda-Yamamoto,‡ Naoki Inagaki,§ Hiroichi Nagai,§ Yoshinori Yamanishi,* Hideaki Nakajina,* Hidetoshi Kumagai,* and Toshio Kitamura[2]*

Integrin α_{IIb}, a well-known marker of megakaryocyte-platelet lineage, has been recently recognized on hemopoietic progenitors. We now demonstrate that integrin $\alpha_{IIb}\beta_3$ is highly expressed on mouse and human mast cells including mouse bone marrow-derived mast cells, peritoneal mast cells, and human cord blood-derived mast cells, and that its binding to extracellular matrix proteins leads to enhancement of biological functions of mast cells in concert with various stimuli. With exposure to various stimuli, including cross-linking of FcεRI and stem cell factor, mast cells adhered to extracellular matrix proteins such as fibrinogen and von Willebrand factor in an integrin $\alpha_{IIb}\beta_3$-dependent manner. In addition, the binding of mast cells to fibrinogen enhanced proliferation, cytokine production, and migration and induced uptake of soluble fibrinogen in response to stem cell factor stimulation, implicating integrin $\alpha_{IIb}\beta_3$ in a variety of mast cell functions. In conclusion, mouse and human mast cells express functional integrin $\alpha_{IIb}\beta_3$. *The Journal of Immunology,* 2006, 176: 52–60.

Mast cells, derived from circulating $CD34^+$ hemopoietic progenitor cells, differentiate and proliferate in vascularized tissues. These steps are critically regulated by stem cell factor (SCF),[3] the ligand for c-*kit*, which is a receptor tyrosine kinase expressed on the surface of mast cells (1, 2) as well as immature hemopoietic cells.

It is widely accepted that mast cells play a critical role in IgE-mediated immune reactions such as immediate hypersensitivity; mast cells are activated by cross-linking of Ag-specific IgE bound to FcεRI with a multivalent specific Ag. Mast cells secrete preformed and newly synthesized proinflammatory mediators such as histamine, lipids, and cytokines (1–3). In addition, some sets of monomeric IgE molecules, termed high cytokinergenic (HC) IgE, can also activate mast cells and induce a similar response without specific Ags (1, 4, 5).

In contrast, mast cells also participate in a wide variety of pathological processes independent of IgE, including innate immune response (1, 2, 6), tissue repair (1, 2, 7), acute inflammatory response to implanted biomaterials (8), atherosclerosis (9), and certain autoimmune disorders (10).

Under both IgE-dependent and -independent pathological conditions, cell-extracellular matrix (ECM) interactions mediated by integrins play crucial roles in a variety of mast cell functions such as histamine release (11), cytokine production (3, 5), survival (5), growth (12), and migration (13, 14).

Integrins are heterodimeric type I transmembrane receptors composed of two subunits (α and β). Integrin α_{IIb}, recently proven to be a marker for early hemopoietic progenitors (15), was considered to be expressed exclusively on megakaryocyte-platelet lineage as a complex with integrin β_3 to form integrin $\alpha_{IIb}\beta_3$, also called glycoprotein IIb-IIIa or CD41-CD61, whereas integrin β_3 is present on many types of cells as a complex with integrin α_V. In platelets, integrin $\alpha_{IIb}\beta_3$ works as a receptor for fibrinogen, von Willebrand factor (vWF), vitronectin (VN), fibronectin (FN), CD40L, and others (16). Integrin $\alpha_{IIb}\beta_3$ links platelets to the injured sites of vessels through interaction with fibrinogen and vWF, together with an aggregate to form a platelet plug, leading to hemostasis (16–21). Eventually, fibrinogen is internalized and stored in granules of megakaryocytes and platelets (22–25).

The activation of bone marrow-derived mast cell (BMMC) with various stimuli, including IgE and Ag (this mode of stimulation termed IgE plus Ag) (1, 2, 11, 18, 26), monomeric IgE (1, 5, 27), SCF (28, 29), and thrombin (30) induces the adhesion to FN predominantly via integrin $\alpha_5\beta_1$. BMMC stimulated by TGF-β adhere to laminin-1 via integrin α_7 (31), whereas adhesion of BMMC to VN is mediated by integrin $\alpha_V\beta_3$ (12). IgE plus Ag-stimulated peritoneal mast cells (PMC), but not BMMC, adhere to type I collagen via integrin $\alpha_2\beta_1$ (32). However, functions of integrin $\alpha_{IIb}\beta_3$ have never been addressed in mast cells.

In the present work, we demonstrate that integrin $\alpha_{IIb}\beta_3$ is highly expressed on mast cells using mouse BMMC, PMC, and human cord blood- derived mast cells. We also found that mast cells stimulated by various stimuli adhere to ECM protein such as fibrinogen and vWF in an integrin $\alpha_{IIb}\beta_3$-dependent manner. Moreover, the interaction of integrin $\alpha_{IIb}\beta_3$ to fibrinogen enhances mast cell functions and induces uptake of fibrinogen into mast cells. Considering that several drugs regulate the function of integrin

*Division of Cellular Therapy and Division of Hematopoietic Factors, Advanced Clinical Research Center, and †Laboratory of Stem Cell Therapy, Center for Experimental Medicine, Institute of Medical Science, University of Tokyo, Tokyo, Japan; ‡National Institute of Vegetable and Tea Science, National Agriculture Research Organization, Shizuoka, Japan; and §Department of Pharmacology, Gifu Pharmaceutical University, Gifu, Japan

Received for publication May 20, 2005. Accepted for publication October 10, 2005.

The costs of publication of this article were defrayed in part by the payment of page charges. This article must therefore be hereby marked *advertisement* in accordance with 18 U.S.C. Section 1734 solely to indicate this fact.

[1] This study was supported by the Ministry of Education, Science, Technology, Sports and Culture and the Ministry of Health and Welfare, Japan. The Division of Hematopoietic Factors is supported by the Chugai Pharmaceutical Company, Tokyo, Japan.

[2] Address correspondence and reprint requests to Dr. Toshio Kitamura, Division of Cellular Therapy, Advanced Clinical Research Center, Institute of Medical Science, University of Tokyo, 4-6-1 Shirokanedai, Minato-ku, Tokyo 108-8039, Japan. E-mail address: kitamura@ims.u-tokyo.ac.jp

[3] Abbreviations used in this paper: SCF, stem cell factor; HC, high cytokinergenic; ECM, extracellular matrix; BMMC, bone marrow-derived mast cell; PMC, peritoneal mast cell; vWF, von Willebrand factor; VN, vitronectin; FN, fibronectin.

0022-1767/05/$02.00

$\alpha_{IIb}\beta_3$ (33), these results might provide a feasible way to overcome mast cell-mediated disorders.

Materials and Methods

Abs and other materials

The source of Abs are as described. Anti-mouse integrin $\alpha_{IIb}\beta_3$ mAb (1B5) was a gift from Dr. B. S. Coller (Rockefeller University, New York, NY) (34). Anti-mouse integrin α_V (8B3) and anti-mouse integrin β_3 (8B11) mAbs were gifts from Drs. D. J. Gerber and S. Tonegawa (Picower Center, Massachusetts Institute of Technology, Boston, MA) (35). Anti-human integrin $\alpha_{IIb}\beta_3$ mAb (2G12) was a gift from Dr. V. L. Woods (University of California, San Diego, CA) (36). Anti-DNP IgE (SPE-7) was from Sigma-Aldrich. Anti-TNP IgE (C38-2), anti-mouse integrin α_{IIb} (MWReg30), anti-mouse integrin α_V (RMV-7 and H9.2B8), anti-mouse integrin α_4 (9C10), anti-mouse integrin α_5 (5H10-27), anti-mouse LFA1 (M17/4), anti-mouse integrin β_1 (Ha2/5), anti-mouse integrin β_2 (GAME-46), and anti-mouse integrin $\alpha_V\beta_3$ (2C9.G2) mAbs, and others were from BD Biosciences. Cytokines such as mouse IL-3 and SCF were obtained from R&D Systems. Thrombin, bovine serum VN, and DNP-BSA were from Sigma-Aldrich, and human plasma fibrinogen and vWF were from Chemicon International. Human fibrinogen labeled with Alexa Fluor 488 was purchased from Molecular Probes.

Cells

To generate BMMC with 90% purity (c-*kit*$^+$/FcϵRI$^+$ by flow cytometry), bone marrow cells from 6-wk-old male BALB/c or C57BL/6 or CBA mice (Charles River Laboratories) were cultured for 4–8 wk in RPMI 1640/10% FCS supplemented with 2-ME and 10 ng/ml IL-3 (BMMC culture medium).

PMC were generated from peritoneal cells, as described previously (37, 38). In brief, mononuclear cells collected from peritoneal lavage were cultured for 10–14 days in the presence of 10 ng/ml IL-3 and 30 ng/ml SCF, and PMC with 90% purity were obtained.

Skin-derived mast cells were generated from day 16 fetal skin of mice as described (39, 40). Briefly, excised trunk skin was treated with 0.25% of trypsin in HBSS for 30 min at 37°C, and the dispersed cells were cultured in the medium containing 10% FCS, 10 ng/ml IL-3, and 30 ng/ml SCF for 14 days.

Lung-derived mast cells were generated from lung tissue samples of adult mice as described (41). Briefly, the samples were cut into fragments and digested with collagenase and hyaluronidase. The single cell suspension were prepared and cultured in the medium containing 10% of FCS, 10 ng/ml IL-3, and 30 ng/ml SCF for 14 days.

Human cord blood-derived mast cells were generated from CD34$^+$ cord blood cells, as described (42). Mast cells with 90% purity were generated by 8 wk of culture in the medium containing 10% FCS, 100 ng/ml human SCF, and 50 ng/ml human IL-6. Megakaryocytes were generated, as described previously (43). Animal and human studies were approved by the animal care committee and the ethical committee of the Institute of Medical Science, University of Tokyo (Tokyo, Japan).

Bone marrow-derived basophils were prepared as described (44). In brief, bone marrow cells were cultured for 10 days in the presence of 10 ng/ml IL-3. Approximately 30% of the cells were FcϵRI$^+$/c-*kit*$^-$ population, which were mainly composed of basophils.

FACS analysis

Cells (3×10^5 cells) were suspended in 2% FCS/PBS, blocked with mouse FcBlock (BD Biosciences), washed with 2% FCS/PBS, incubated with 20 μg/ml primary Abs for 20 min at 4°C, washed twice, incubated with 20 μg/ml secondary Abs for 20 min, washed twice again, then resuspended in 2% FCS/PBS. The samples were then analyzed using a FACSCalibur flow cytometer (BD Biosciences).

RT-PCR

Total RNA was prepared from freshly isolated cells with TRIzol (Invitrogen Life Technologies). Total RNA from each sample was reverse transcribed with SuperScript Reverse Transcriptase kit (Qiagen) and oligo(dT) primer. The primer used for integrin α_{IIb} in this study was as described previously (45)

Immunoprecipitation assay

Ten million cells of BMMC and BW1457 were surface biotinylated, collected, and lysed in a radioimmunoprecipitation assay buffer. The lysates were immunoprecipitated with a control Ab (hamster IgG or rat IgG) or anti-mouse integrin α_{IIb} Abs (1B5 or MWReg30) or an anti-mouse integrin $\alpha_V\beta_3$ Ab (2C9.G2). Immunoprecipitates were run on 7.5% SDS-PAGE gels and transferred to Immobilon membranes. The membranes were blotted using HRP-conjugated streptavidin.

Adhesion assay

Adhesion assay was done as described previously (28). In brief, the 96-well plates (no. 3631; Corning) were coated with 20 or 50 μg/ml VN, vWF, or fibrinogen in PBS for 1 h at 37°C, and washed three times with PBS, followed by blocking with 3% BSA/PBS for 1 h at 37°C and washing three times with RPMI 1640 containing 10 mM HEPES and 0.03% BSA (the assay medium). BMMC, washed four times in the assay medium, were resuspended at 5×10^5 cells/ml in the assay medium and transferred into coated wells (100 μl/well) with or without stimulant including IgE (SPE-7), DNP-BSA (for IgE plus Ag), SCF, and thrombin with the indicated concentration for 1 h at 37°C. For stimulation with IgE plus Ag, BMMC were pretreated with 0.5 μg/ml IgE (C38-2) overnight at 37°C. After washing, cell adhesion was quantitated using CellTiter-Glo (Promega) and a Micro Lumat Plus luminometer (EG&G Berthold), according to the manufacturer's instructions.

In assays using blocking Abs, BMMC were preincubated with 10–50 μg/ml Abs for 1 h before adding the cells to the plate.

Migration assay

Migration assays were conducted, as previously described (13), using 24-well Transwell chambers with 5-μm polycarbonate filters (Corning). Briefly, the underside of each insert was treated with 30 μg/ml FN or 50 μg/ml fibrinogen for 1 h at 37°C, blocked with 3% BSA/PBS for 1 h at 37°C, then placed back in the Transwell lower chamber containing 0.5 ml of the assay medium, with or without stimulants such as SCF. The washed cells resuspended at 7.5×10^7 cells/ml in 0.2 ml of the assay medium were transferred to the insert. After incubating them for 8 h at 37°C, the cells migrated to lower chambers were counted using a hematocytometer.

Cytokine assay (ELISA)

The cells were transferred into FN- or fibrinogen-coated 96-well plates (1×10^4 cells/well) with or without stimulants. After incubating for 12 h at 37°C, the supernatant of each well was collected, and the concentration of IL-6 was quantified by ELISA with OptiEIA for IL-6 (BD Pharmingen).

Growth assay

The cells were resuspended at 3×10^5 cells/ml in a BMMC culture medium with IL-3, and transferred into fibrinogen-coated 24-well plates with or without SCF. After incubation for the indicated time period at 37°C, the cells were collected and counted using a hematocytometer.

Induced uptake of fibrinogen into SCF-stimulated mast cells

BMMC were suspended at 5×10^5 cells/ml in a Tyrode's buffer with 10 μg/ml of a control Ab or the anti-integrin $\alpha_{IIb}\beta_3$ Ab (1B5). Cell were then incubated for 30 min at room temperature, and incubated with 20 μg/ml fibrinogen labeled with Alexa Fluor 488 in the presence of 100 ng/ml SCF or PBS for 30 min at room temperature. After washing, the cells were analyzed using FACS or a confocal microscope (Olympus Tokyo). For confocal microscopy, the cells attached to microscope slides were fixed with 4% paraformaldehyde, stained with 4′,6′-diamidino-2-phenylindole, and then visualized.

Results

BMMC and PMC express integrin $\alpha_{IIb}\beta_3$

We first tested the expression of integrins on two different types of mast cells, BMMC and PMC (Fig. 1, *A* and *B*), both of which were >90% FcϵRI$^+$/c-*kit*$^+$ using flow cytometric analysis. We confirmed the expression of integrin α_4 (11, 13, 30, 46, 47), α_5 (5, 11, 26, 28, 30), α_V (12), α_L (48, 49), β_1 (11, 26), β_2 (50), and β_3 (12), as reported (Fig. 1*A*). Interestingly, the expression of integrin α_{IIb} was evident on both BMMC and PMC in FACS and RT-PCR (Fig. 1, *A* and *B*), the expression level being higher in the former. The expression was not due to megakaryocyte progenitors contaminated in our BMMC preparation because we did not detect a megakaryocyte-specific marker, GPIb-a, GPIb-b, or GPV, in our BMMCs (Fig. 1*A* and data not shown). We also confirmed the expression on other types of mast cells, such as skin- and lung-derived mast cells (Fig. 1*C*). As integrin α_{IIb} heterodimerized

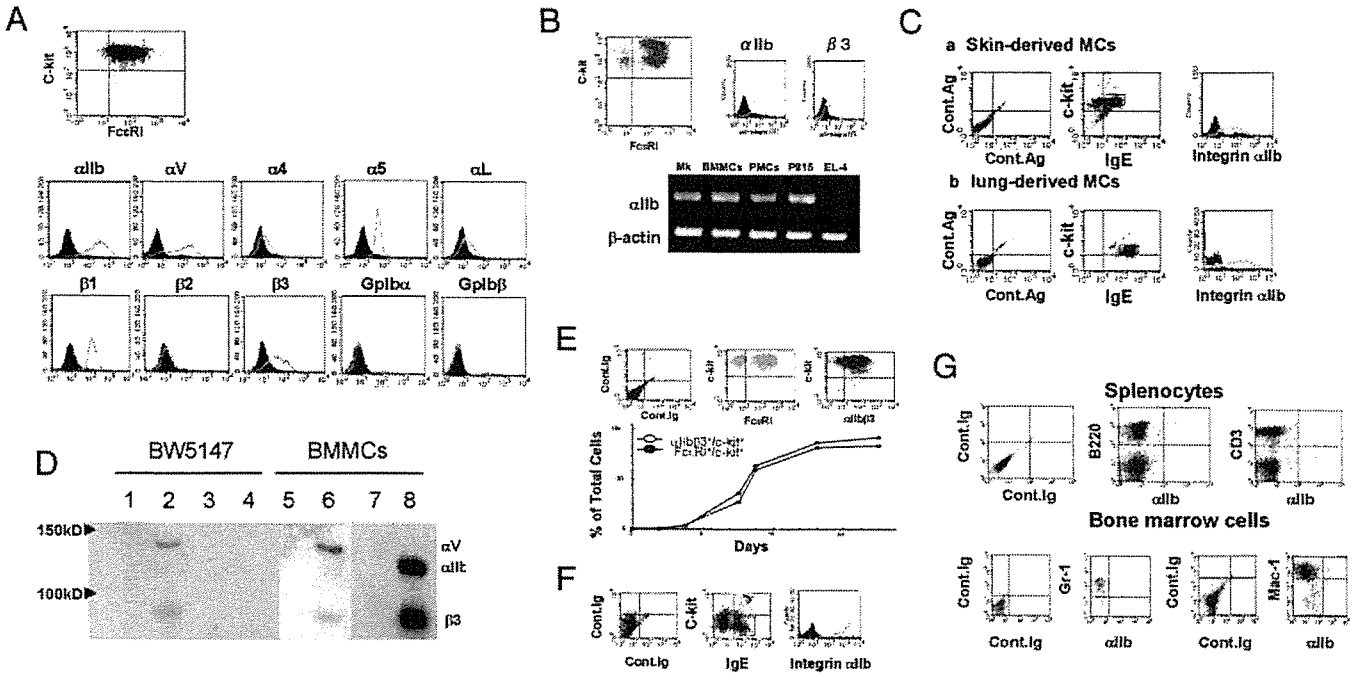

FIGURE 1. Surface expression of integrin $\alpha_{IIb}\beta_3$ was detected on mouse mast cells. *A*, BMMC with >90% purity (FcεRI$^+$/c-*kit*$^+$) expressed integrin α_{IIb} as well as integrins α_V, α_4, α_5, α_L, β_1, β_2, β_3 on BMMC, but not platelet-specific markers GPIb-α or GPIb-β. The *x*-axis indicates fluorescence intensity as a log scale ranging from 10^0 to 10^4. The *y*-axis indicates the number of the cells. *B*, PMC with 90% purity (FcεRI$^+$/c-*kit*$^+$) also expressed integrin α_{IIb} and β_3. RT-PCR confirmed the expression of integrin α_{IIb} in BMMC, PMC, and P815, a mast cell line, but not in EL-4, a T cell line. *C*, Skin- and lung-derived mast cells expressed integrin α_{IIb}. *D*, Both integrin $\alpha_{IIb}\beta_3$ and integrin $\alpha_V\beta_3$ were expressed on the surface of BMMC, whereas only integrin $\alpha_V\beta_3$ was expressed on BW5147. The cell lysates of surface biotinylated BMMC and BW5147 were immunoprecipitated with control Ab (*lanes 1, 3, 5,* and *7*) or the Abs against integrin $\alpha_V\beta_3$ (*lanes 2* and *6*) or $\alpha_{IIb}\beta_3$ (*lanes 4* and *8*), then analyzed with HRP-conjugated streptavidin. *E*, The expression of integrin α_{IIb} on bone marrow-derived cells after different times of culture in the presence of IL-3 was also analyzed using flow cytometry. Dot plot shows FcεRI$^+$/c-*kit*$^+$ and $\alpha_{IIb}{}^+$/c-*kit*$^+$ cells on day 28. *F*, The expression of integrin α_{IIb} was observed on bone marrow-derived basophils. *G*, The expression of integrin α_{IIb} on B220$^+$ splenocytes, CD3$^+$ splenocytes, Gr-1$^+$ bone marrow cells, and Mac-1$^+$ bone marrow cells was not detected in FACS analysis.

solely with integrin β_3, integrin $\alpha_{IIb}\beta_3$ was expected to be expressed on mouse mast cells. To verify integrin $\alpha_{IIb}\beta_3$ expression, BMMC and BW5147 expressing only integrin $\alpha_V\beta_3$ were surface-labeled by biotin and immunoprecipitated with a specific Ab against integrin $\alpha_{IIb}\beta_3$ (1B5). Western blots developed with HRP-conjugated streptavidin gave two bands corresponding to integrin α_{IIb} and β_3 only in the precipitates from BMMC but not from BW5147, suggesting that mouse mast cells express integrin $\alpha_{IIb}\beta_3$ on the cell surface (Fig. 1*D*).

Next, the expression levels of integrin α_{IIb} were examined on BMMC in the course of culture with IL-3, that is, in the varying developmental stages toward BMMC. The percentage of $\alpha_{IIb}{}^+$/c-*kit*$^+$ cells gradually increased during the culture in parallel with increase in the percentage of FcεRI$^+$/c-*kit*$^+$ cells indicative of mast cells or mast cell progenitors, and reached ~90% after 28 days (Fig. 1*E*).

Interestingly, FcεRI$^+$/c-*kit*$^-$ cells, which were mainly composed of bone marrow-derived basophils, expressed integrin α_{IIb} at the levels comparable to mast cells (Fig. 1*F*). By contrast, no or negligible expression of integrin α_{IIb} was observed on T cells (CD3$^+$ splenocytes), B cells (B220$^+$ splenocytes), granulocytes (Gr-1$^+$ bone marrow cells), macrophages (Mac-1$^+$ bone marrow cells, bone marrow-derived macrophages, and peritoneal macrophages), and dendritic cells (bone marrow-derived dendritic cells) (Fig. 1*G* and data not shown). These results suggest that the expression of integrin α_{IIb} on cells other than megakaryocytes/platelets was limited to mast cells.

Adhesion of mast cells to immobilized fibrinogen- and vWF-mediated by integrin $\alpha_{IIb}\beta_3$

As integrin $\alpha_{IIb}\beta_3$ works as a receptor for ECM proteins, such as fibrinogen, vWF, VN, and FN in megakaryocytes and platelets, we examined whether mast cells expressing integrin $\alpha_{IIb}\beta_3$ could adhere to these ECM proteins.

Although nonstimulated BMMC did not significantly bind to any ECM proteins, BMMC stimulated by monomeric HC IgE (SPE-7) adhered to all of the ECM proteins (Fig. 2, *A* and *B*). Integrin $\alpha_{IIb}\beta_3$ on platelets could interact with all these ECM proteins, but several studies revealed that the adhesion of mast cells to FN and VN was mainly mediated by integrin $\alpha_5\beta_1$ (5, 11, 28–31) and $\alpha_V\beta_3$ (12), respectively.

To clarify the involvement of each integrin in mast cell adhesion to ECM proteins, we used specific blocking Abs against integrin $\alpha_{IIb}\beta_3$ (anti-integrin $\alpha_{IIb}\beta_3$ Ab), 1B5 and $\alpha_V\beta3$ (anti-integrin $\alpha_V\beta_3$ Ab), 2C9.G2. A hamster mAb, 1B5, raised against mouse integrin $\alpha_{IIb}\beta_3$, specifically recognizes mouse integrin $\alpha_{IIb}\beta_3$ and completely blocks platelet-fibrinogen interaction, thereby inhibiting platelet aggregation (34). On the contrary, 2C9.G2, a hamster mAb against mouse integrin $\alpha_V\beta_3$, reacts with integrin β_3 in FACS analysis and blocks the adhesion via integrin $\alpha_V\beta_3$ (11, 51).

BMMC were pretreated with specific blocking Abs, anti-integrin $\alpha_{IIb}\beta_3$ Ab, anti-integrin $\alpha_V\beta_3$ Ab, or anti-integrin β_1 Ab, Ha2/5, before the adhesion assay. As shown in Fig. 2, *A* and *B*, anti-integrin $\alpha_{IIb}\beta_3$ Ab inhibited 90% of the adhesion of mast cells to fibrinogen and 70% of adhesion to vWF, whereas it only weakly inhibited of the adhesion to VN. On the contrary, the

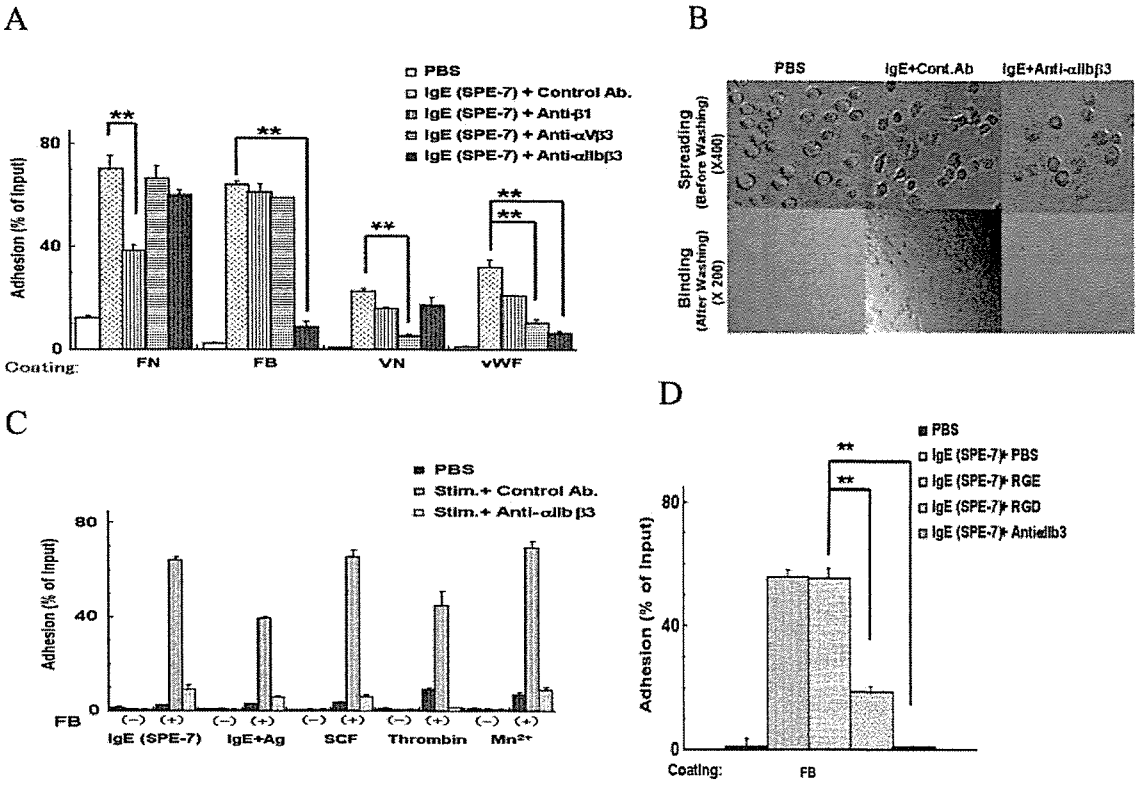

FIGURE 2. Integrin $\alpha_{IIb}\beta_3$ on stimulated BMMC mediated their adhesion to fibrinogen and vWF. *A* and *B*, Adhesiveness of BMMC stimulated with or without 3 μg/ml HC IgE (SPE-7) for 1 h at 37°C was analyzed on plates coated with or without 20–50 μg/ml ECM proteins (fibrinogen, FN, VN, vWF) by calculating the percentage of the adherent cells (*A*) or by microscope (magnification, ×200 or ×400) (*B*). The results of the functional blockage of integrins with specific anti-integrin Abs (50 μg/ml anti-β_1 Ab, 50 μg/ml anti-integrin $\alpha_V\beta_3$ Ab, 10 μg/ml anti-integrin $\alpha_{IIb}\beta_3$ Ab) are also shown. *C*, The interaction between integrin $\alpha_{IIb}\beta_3$ and fibrinogen was observed in response to stimuli, such as 3 μg/ml IgE (SPE-7), 10 ng/ml DNP-BSA (IgE plus Ag), 100 ng/ml SCF, 1 mM $MnCl_2$, and 10 U/ml thrombin, and was blocked by 10 μg/ml anti-integrin $\alpha_{IIb}\beta_3$ Ab. *D*, Interaction blocked by 100 μg/ml RGD peptides but not by RGE peptides. The results shown are the average ± SD of three independent experiments. **, $p < 1\%$ (vs the control Ab-treated sample determined by Student's *t* test).

anti-integrin $\alpha_V\beta_3$ Ab profoundly inhibited the adhesion of mast cells to VN, whereas it inhibited only 20–30% of the mast cell adhesion to vWF, and did not significantly inhibit that to fibrinogen. The anti-integrin β_1 Ab only partially inhibited mast cell adhesion to VN and vWF, and did not significantly affect that to fibrinogen, indicating that the involvement of integrin β_1 in mast cell adhesion to these ECM proteins was limited. However, binding to FN was inhibited by anti-integrin β_1 Ab but not by anti-integrin $\alpha_{IIb}\beta_3$ Ab or anti-integrin $\alpha_V\beta_3$ Ab, as reported (4, 5, 11, 28–31). Similar results were obtained in experiments using PMC (data not shown). Collectively, these results indicate that the interaction of mast cell with fibrinogen was specifically mediated by integrin $\alpha_{IIb}\beta_3$ and that the interaction of mast cells with VN was mainly mediated by integrin $\alpha_V\beta_3$, as reported (12), but that the efficient adhesion to vWF required both integrin $\alpha_V\beta_3$ and $\alpha_{IIb}\beta_3$.

Characterization of mast cell adhesion to fibrinogen

Next, we asked whether other stimuli could induce the same adhesion, and found that BMMC bound to fibrinogen-coated plates upon stimulation with IgE plus Ag, SCF, thrombin, or Mn^{2+} (Fig. 2*C*)

The interaction of integrin $\alpha_{IIb}\beta_3$ on mast cells to fibrinogen was RGD ((Arg-Gly-Asp)-dependent (Fig. 2*D*) as noted in platelets, and the kinetics of the adhesion induced by HC IgE (SPE-7) and SCF to fibrinogen showed that the adhesion reached a plateau level from 30 to 60 min after the simulation at 37°C (data not shown). As was the case of mast cell adhesion via integrin $\alpha_5\beta_1$ (5, 11, 29), there was no change in the cell surface levels of integrins α_{IIb}, α_V, and β_3 following treatment with these reagents (data not shown). Collectively, these results indicate that adhesion of mast cells to fibrinogen requires inside-out signaling followed by increase in the affinity/avidity of integrin $\alpha_{IIb}\beta_3$.

SCF induced integrin $\alpha_{IIb}\beta_3$-directed migration of mast cells

Accumulating evidence revealed that several kinds of integrins were involved in the migration of mast cells (13, 37, 47, 50), and that the interaction between SCF and c-*kit* regulated the migration of mast cells via ECM proteins, especially FN (13, 14, 37, 47, 50, 52). We examined SCF-induced migration of mast cells via fibrinogen, and then tested whether integrin $\alpha_{IIb}\beta_3$-fibrinogen interaction would induce migration.

As shown in Fig. 3*A*, the number of migrated BMMC were 5-fold higher via the fibrinogen-treated Transwell membrane surface than the BSA-treated surface in the presence of SCF in the lower wells, and this enhancement was significantly blocked by anti-integrin $\alpha_{IIb}\beta_3$ Ab, indicating that SCF enhances migration via fibrinogen in an integrin $\alpha_{IIb}\beta_3$-dependent manner.

Effects of mast cell-fibrinogen interaction on mast cell functions

Adhesion of mast cells to FN was reported to enhance mast cell functions, such as production of IL-6 or TNF-α (28), proliferation (12), survival (28), and histamine release (5). We tested whether

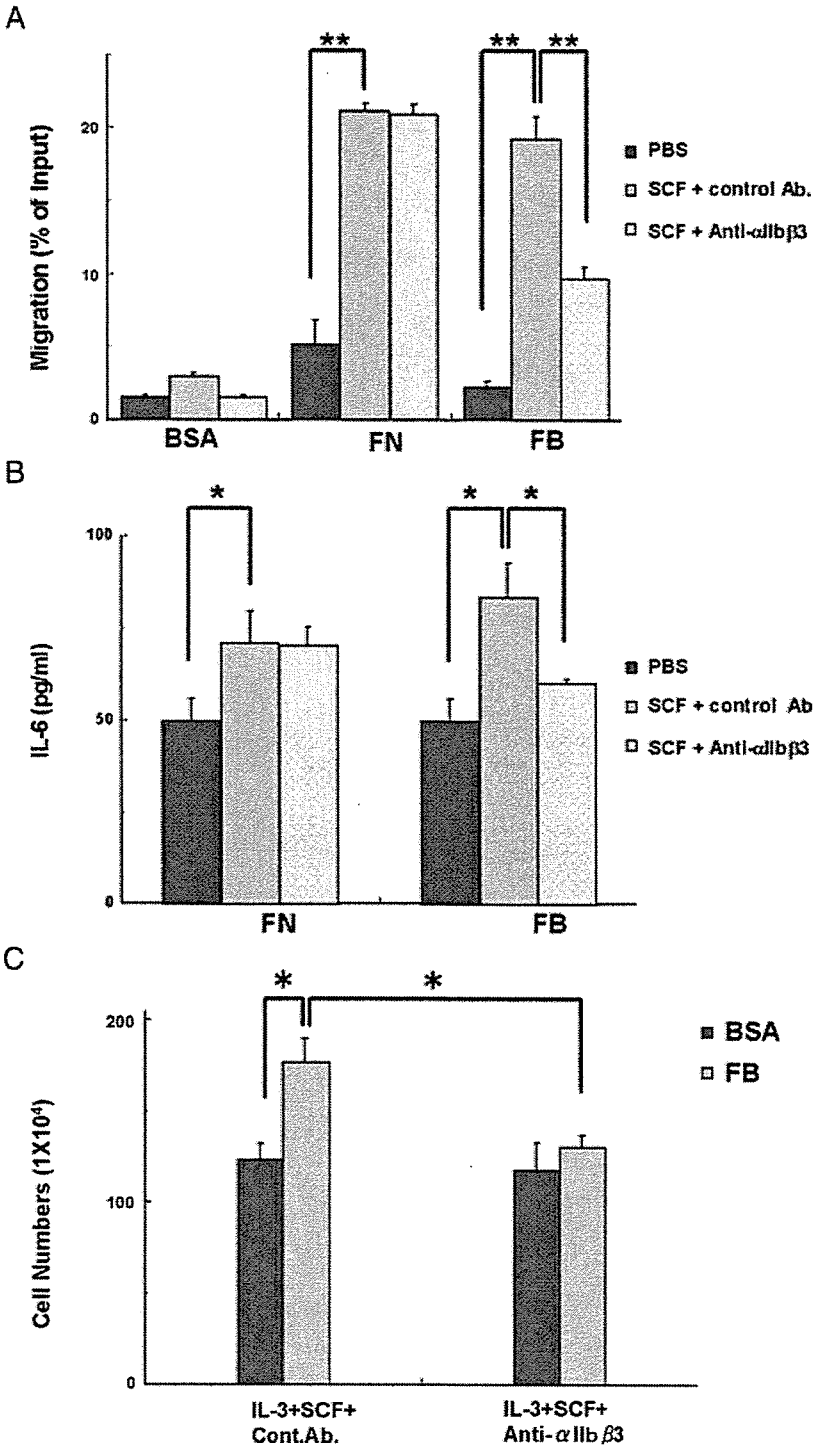

FIGURE 3. Integrin $\alpha_{IIb}\beta_3$ enhanced mast cell function. *A*, BMMC in upper wells were attracted by 100 ng/ml SCF in lower wells, much more efficiently through fibrinogen or FN-treated Transwell than a BSA-treated surface in an 8-h assay. This enhancement was blocked by 10 μg/ml anti-integrin $\alpha_{IIb}\beta_3$. *B*, BMMC stimulated with 100 ng/ml SCF for 12 h produced IL-6 on FN- or fibrinogen-treated plates. The concentration of IL-6 in culture supernatants was quantified by ELISA. IL-6 production was enhanced on fibrinogen-coated plates, and the enhancement was significantly blocked by 10 μg/ml anti-integrin $\alpha_{IIb}\beta_3$ Ab. *C*, The number of BMMC after 7 days of culture in the presence of 10 ng/ml IL-3 and 100 ng/ml SCF was augmented on fibrinogen-coated plates and significantly blocked with 10 μg/ml anti-integrin $\alpha_{IIb}\beta_3$ Abs. The results shown are the average ± SD of three independent experiments. *, $p < 5\%$ and **, $p < 1\%$ (vs the cells incubated in BSA-coated plates or the control Ab-treated cells, respectively, as determined by Student's *t* test).

mast cell adhesion to fibrinogen had any effects on mast cell functions: IL-6 production, growth, and survival and histamine release.

First, IL-6 production was measured using ELISA. BMMC attached to fibrinogen-coated plates produced 50% larger concentrations of IL-6 than those on BSA-coated plates in response to SCF or thrombin, and this enhancement of IL-6 production was clearly blocked by anti-integrin $\alpha_{IIb}\beta_3$ Ab, indicating the interaction between integrin $\alpha_{IIb}\beta_3$ and fibrinogen enhances IL-6 production of mast cells (Fig. 3*B*). In contrast, histamine release from BMMC was not enhanced by the interaction with fibrinogen via the integrin (data not shown).

Second, growth and survival of mast cells was examined. The number of BMMC on fibrinogen-coated plates was 45% higher than that on BSA-coated plates after 1 wk of culture, and this increment was also dependent on integrin $\alpha_{IIb}\beta_3$ (Fig. 3*C*). However, we could not find the effects of the binding to fibrinogen on the differentiation of BMMC or bone marrow cells cultured with IL-3 plus SCF (data not shown).

SCF-induced survival was estimated by measuring the percentage of apoptotic cells, induced by the withdrawal of IL-3. However, no significant difference was found between BMMC on fibrinogen-coated and BSA-coated plates in the presence of SCF